

On the Dynamics of the Tavis-Cummings Model

Zhiyuan Dong, Guofeng Zhang, Ai-Guo Wu, and Re-Bing Wu

Abstract—The purpose of this paper is to present a comprehensive study of the Tavis-Cummings model from a system-theoretic perspective. A typical form of the Tavis-Cummings model is composed of an ensemble of non-interacting two-level systems (TLSs) that are collectively coupled to a common cavity resonator. The associated quantum linear passive system is proposed, whose canonical form reveals typical features of the Tavis-Cummings model, including \sqrt{N} -scaling, dark states, bright states, single-excitation superradiant and subradiant states. The passivity of this linear system is related to the vacuum Rabi mode splitting phenomenon in Tavis-Cummings systems. On the basis of the linear model, an analytic form is presented for the steady-state output state of the Tavis-Cummings model driven by a single-photon state. Master equations are used to study the excitation properties of the Tavis-Cummings model in the multi-excitation scenario. Finally, in terms of the transition matrix for a linear time-varying system, a computational framework is proposed for calculating the state of the Tavis-Cummings model, which is applicable to the multi-excitation case.

Index Terms—Quantum control, Tavis-Cummings model, two-level systems, open quantum systems.

I. INTRODUCTION

In 1954, Robert Dicke calculated [1] that an ensemble of gaseous molecules interacting with a common radiation field could exhibit a coherent spontaneous emission process, during which the molecules act as a giant molecule that shows super-radiation — cooperative radiation rate much faster than independent individual radiation rates. This problem was further studied by Tavis and Cummings [2] by means of a model of N identical non-interacting two-level systems (TLSs) coupled to a single-mode quantized radiation field, see Fig. 1 in section III for an example. An exact solution of the eigenstates of the Hamiltonian for this model is derived. The model proposed in [2] is called the Tavis-Cummings model in the subsequent literature. The Tavis-Cummings model has been physically realized by quite a few experimental platforms, including superconducting circuits [3]–[6], NV spin ensembles [7], and double quantum dots [8]–[10]. In the Tavis-Cummings model consisting of N TLSs equally coupled to a cavity resonator, under certain conditions the collective coupling strength of the ensemble exhibits a \sqrt{N} -scaling, which can be experimentally observed from the vacuum Rabi mode splitting of the resonator

transmission spectrum of the bright states. In addition to bright states, a Tavis-Cummings model can also have dark states which contain single-excitation subradiant states as a subclass. Applications of the Tavis-Cummings model can be found in [4], [6], [9], [11] and references therein.

In this paper, we aim to introduce the Tavis-Cummings model to the quantum control community and show that many of its typical properties can be uncovered by means of systems theory. The main contributions are summarized below.

In section III-B we propose a quantum linear system that is associated to the Tavis-Cummings model. This linear model reveals the \sqrt{N} -scaling of the coupling strength of the atomic ensemble. Moreover, a transfer function is defined for a performance variable for which the system is passive, and the transfer function reflects the vacuum Rabi mode splitting of the Tavis-Cummings model. Finally, the structural decomposition of the linear model shows that the bright states of the Tavis-Cummings model live in the controllable and observable subspace, whereas the dark states reside in the uncontrollable and unobservable subspace of the linear model.

In section IV-A we apply the quantum linear systems theory to derive an analytic form of the output single-photon state of the Tavis-Cummings system driven by a single-photon input. The simulations in Fig. 2 show that the input photon tends not to interact with the atoms when the number of atoms is large, and photon-atom interaction is easier when atoms are non-resonant. On the other hand, when only one of the two-level atoms is initially excited and the input field is vacuum, an analytic form of the joint system-field state is given in section IV-C, which explains several experimental observations including superradiance and subradiance [6].

In section V, we study the excitations of TLSs by means of master equations. When all the N atoms are initially in the excited state, we prove that eventually they all settle to the ground state and the output field is in an N -photon state, provided that the coupling strengths are identical.

In our preliminary study [13], a computational framework is proposed to calculate the joint system-field state of a general open quantum system. Here, we develop it further in section VI and apply it to the study of the Tavis-Cummings model. In particular, we derive the exact form of 2- and 3-photon states.

Notation. The reduced Planck constant \hbar is set to 1. $i = \sqrt{-1}$ is the imaginary unit, δ_{ij} denotes the Kronecker delta function, and $\delta(t - r)$ is the Dirac delta function. I is the identity matrix, and $\mathbf{0}$ is the zero vector or matrix whose dimension can be easily determined from the context. Given a column vector of complex numbers or operators $X = [x_1, \dots, x_n]^T$, the complex conjugate or adjoint operator of X is denoted by $X^\# = [x_1^*, \dots, x_n^*]^T$. Let $X^\dagger = (X^\#)^T$. Clearly, when $n = 1$, $X^\dagger = X^*$. Let t_0 be the initial time, i.e., the time when the system and its input start interaction.

Zhiyuan Dong is with School of Science, Harbin Institute of Technology, Shenzhen, Shenzhen, China (e-mail: dongzhiyuan@hit.edu.cn).

Guofeng Zhang is with the Department of Applied Mathematics, The Hong Kong Polytechnic University, Hong Kong. He is also with The Hong Kong Polytechnic University Shenzhen Research Institute, Shenzhen, 518057, China (e-mail: guofeng.zhang@polyu.edu.hk).

Ai-Guo Wu is with School of Mechanical Engineering and Automation, Harbin Institute of Technology, Shenzhen, Shenzhen, China (e-mail: agwu@hit.edu.cn, ag.wu@163.com).

Re-Bing Wu is with the Center for Intelligent and Networked Systems, Department of Automation, Tsinghua University, Beijing, 100084, China (e-mail: rbwu@tsinghua.edu.cn).

$|g\rangle$ and $|e\rangle$ stand for the ground and excited states of a two-level atom, respectively. The commutator between two operators A and B is $[A, B] = AB - BA$. Define superoperators $\mathcal{L}X \triangleq -i[X, H] + \mathcal{D}_L X$ and $\mathcal{L}^* \rho \triangleq -i[H, \rho] + \mathcal{D}_L^* \rho$, where $\mathcal{D}_L X = L^\dagger X L - \frac{1}{2} L^\dagger L X - \frac{1}{2} X L^\dagger L$ and $\mathcal{D}_L^* \rho = L \rho L^\dagger - \frac{1}{2} L^\dagger L \rho - \frac{1}{2} \rho L^\dagger L$.

II. PRELIMINARIES

A. Quantum systems and fields

Consider a quantum system driven by m input fields. The inputs are optical or microwave fields, which are represented by the annihilation operators $b_{\text{in},k}(t)$ and their adjoints $b_{\text{in},k}^*(t)$ (creation operators), $k = 1, \dots, m$. If there are no photons in an input channel, this input is in the vacuum state $|\Phi_0\rangle$. Annihilation and creation operators satisfy

$$b_{\text{in},j}(t)|\Phi_0\rangle = 0, [b_{\text{in},j}(t), b_{\text{in},k}(r)] = [b_{\text{in},j}^*(t), b_{\text{in},k}^*(r)] = 0, [b_{\text{in},j}(t), b_{\text{in},k}^*(r)] = \delta_{jk}\delta(t-r), \forall j, k = 1, \dots, m, t, r \in \mathbb{R}. \quad (1)$$

The integrated input annihilation and creation processes are respectively $B_{\text{in},k}(t) = \int_{-\infty}^t b_{\text{in},k}(r)dr$ and $B_{\text{in},k}^*(t) = \int_{-\infty}^t b_{\text{in},k}^*(r)dr$, which are quantum Wiener processes. Define Itô increments $dB_{\text{in},k}(t) = B_{\text{in},k}(t+dt) - B_{\text{in},k}(t)$. Denote $B_{\text{in}}(t) = [B_{\text{in},1}(t), \dots, B_{\text{in},m}(t)]^\top$. In this paper, the input fields are assumed to be canonical fields which include the vacuum, coherent, single- and multi-photon fields. Then $dB_{\text{in}}(t)dB_{\text{in}}^\top(\tau) = dB_{\text{in}}^\#(t)dB_{\text{in}}^\dagger(\tau) = dB_{\text{in}}^\#(t)dB_{\text{in}}^\top(\tau) = \mathbf{0}$ and $dB_{\text{in}}(t)dB_{\text{in}}^\dagger(\tau) = I\delta_{t\tau}dt$.

The quantum system can be parametrized by a triple (S, L, H) [15], [16]. Here, H is the inherent system Hamiltonian, $L = [L_1, \dots, L_m]^\top$ describes how the system is coupled to its environment, and S is a scattering operator (e.g., a beamsplitter or a phase shifter). In this paper, it is assumed that $S = I$ (the identity operator). The temporal evolution of the quantum system is governed by a unitary operator $U(t, t_0)$, which is the solution to the following Itô quantum stochastic differential equation (QSDE):

$$dU(t, t_0) = \left[-(iH + \frac{1}{2}L^\dagger L)dt + dB_{\text{in}}^\dagger(t)L - L^\dagger dB_{\text{in}}(t) \right] U(t, t_0)$$

under the initial condition $U(t_0, t_0) = I$. Denote the joint system-field state by $|\Psi(t)\rangle$. In the Schrödinger picture, $|\Psi(t)\rangle = U(t, t_0)|\Psi(t_0)\rangle$, which is the solution to the stochastic Schrödinger equation

$$d|\Psi(t)\rangle = \left[-iH_{\text{eff}}dt + dB_{\text{in}}^\dagger(t)L - L^\dagger dB_{\text{in}}(t) \right] |\Psi(t)\rangle, \quad (2)$$

where $H_{\text{eff}} = H - \frac{i}{2}L^\dagger L$ is the effective Hamiltonian that is not self-adjoint [17, Chapter 11]. In particular, if the input fields are initially in the vacuum state $|\Phi_0\rangle$, then (2) reduces to, [17, Chapter 11],

$$d|\Psi(t)\rangle = \left(-iH_{\text{eff}}dt + dB_{\text{in}}^\dagger(t)L \right) |\Psi(t)\rangle. \quad (3)$$

On the other hand, in the Heisenberg picture, the time evolution of the system operator X , denoted by $j_t(X) \equiv X(t) = U^*(t, t_0)(X \otimes I_{\text{field}})U(t, t_0)$, follows the Itô QSDE

$$dj_t(X) = j_t(\mathcal{L}X)dt + \sum_{k=1}^m dB_{\text{in},k}^*(t)j_t([X, L_k]) + \sum_{k=1}^m j_t([L_k^*, X])dB_{\text{in},k}(t).$$

Finally, the output field annihilation operators are $B_{\text{out},k}(t) = U^*(t, t_0)B_{\text{in},k}(t)U(t, t_0)$, ($k = 1, \dots, m$), whose dynamical evolution is $dB_{\text{out}}(t) = L(t)dt + dB_{\text{in}}(t)$. More discussions on open quantum systems can be found in, e.g., [15]–[18].

B. Continuous-mode single-photon states

For each input channel $k = 1, \dots, m$, the creation operator $b_{\text{in},k}^*$ generates a photon from the vacuum. Mathematically, $|1_{k,t}\rangle \triangleq b_{\text{in},k}^*(t)|\Phi_0\rangle$ means a photon is generated at time t in the k th input channel. By (1), $\langle 1_{j,t}|1_{k,\tau}\rangle = \delta_{jk}\delta(t-\tau)$. Hence $\{|1_{k,t}\rangle : t \in \mathbb{R}\}$ is an orthogonal basis of single-photon states for each channel k . Indeed, a single-photon state with temporal pulse shape $\xi(t)$ in the k th channel can be viewed as a superposition of a continuum of $|1_{k,t}\rangle$, i.e.,

$$|1_\xi\rangle = \int_{-\infty}^{\infty} \xi(t)|1_{k,t}\rangle dt = \int_{-\infty}^{\infty} \xi(t)b_{\text{in},k}^*(t)dt|\Phi_0\rangle. \quad (4)$$

Physically, as a quantum state, $|1_\xi\rangle$ can be interpreted in the following way: the probability of finding the photon in the time bin $[t, t+dt]$ is $|\xi(t)|^2 dt$. The normalization condition $\langle 1_\xi|1_\xi\rangle = 1$ requires $\int_{-\infty}^{\infty} |\xi(t)|^2 dt = 1$. As the single-photon state $|1_\xi\rangle$ is parameterized by an L^2 integrable function $\xi(t)$ over \mathbb{C} , it is called a *continuous-mode* single-photon state [21]–[28]. If a single photon is superposed over m channels, then the single-photon state is a superposition state of the form

$$|1_\zeta\rangle = \sum_{k=1}^m \int_{-\infty}^{\infty} \zeta_k(t)|1_{k,t}\rangle dt,$$

whose normalization condition is $\sum_{k=1}^m \int_{-\infty}^{\infty} |\zeta_k(t)|^2 dt = 1$. In particular, if $\zeta_j(t) \equiv 0$ for some $j = 1, \dots, m$, then it means that the input channel j is in the vacuum state and the photon is superposed over the other input channels.

III. THE TAVIS-CUMMINGS MODEL

We first present the Tavis-Cummings model in subsection III-A. In subsection III-B, assuming that the atoms are initially in the ground state, the cavity is empty and the input field is in the vacuum state, we present an associated linear model. Physical interpretation of the linear model is discussed in subsection III-C.

A. The Tavis-Cummings model

In the Tavis-Cummings model as shown in Fig. 1, the N TLSs are not directly coupled to each other; instead, they all couple to the common single-mode cavity. The inherent system

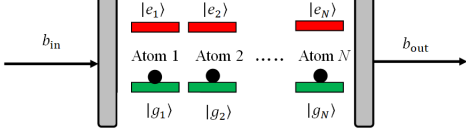


Fig. 1. Schematic of the Tavis-Cummings model. N two-level atoms are coupled to a single-mode cavity, which is driven by an input field. (Here, the atoms are inside the cavity. However, in some physical implementations atoms may be outside the cavity, but of course they must couple to the cavity; see e.g., [9, Fig. 1]). The cavity can also be a transmission line in a superconducting platform.

Hamiltonian of the Tavis-Cummings model is ([2, (2.1)], [3, (1)], [4, (1)], [5, (1)], [9, (C7)], [6, (1)])

$$H_{\text{TC}} = \omega_r a^* a + \sum_{j=1}^N \left[\frac{\omega_j}{2} \sigma_{z,j} + \Gamma_j (a^* \sigma_{-,j} + \sigma_{+,j} a) \right]. \quad (5)$$

Here, a, a^* denote the annihilation and creation operators of the cavity mode satisfying $[a, a^*] = I$, ω_r is the frequency detuning between the cavity mode and the input field. The two-level atom j is coupled to the cavity with coupling strength Γ_j , $j = 1, \dots, N$, which is assumed to a real number but can be negative [5, Table 1] or [7, (2)]. The corresponding detuning between the transition frequency of the two-level atom j and the carrier frequency of the input field is denoted by ω_j . The lowering and raising operators of the two-level atom j are $\sigma_{-,j} = |g_j\rangle\langle e_j|$ and $\sigma_{+,j} = |e_j\rangle\langle g_j|$, respectively. The Pauli Z operator is $\sigma_{z,j} = \sigma_{+,j}\sigma_{-,j} - \sigma_{-,j}\sigma_{+,j}$. The system exchanges information with its environment by means of absorbing and emitting photons, which is realized by the coupling operator $L = \sqrt{\kappa}a$. By the development in subsection II-A, the Itô QSDEs for the Tavis-Cummings model in the Heisenberg picture are

$$\begin{cases} d\sigma_{-,1}(t) = -i\omega_1\sigma_{-,1}(t)dt + i\Gamma_1\sigma_{z,1}(t)a(t)dt, \\ \vdots \\ d\sigma_{-,N}(t) = -i\omega_N\sigma_{-,N}(t)dt + i\Gamma_N\sigma_{z,N}(t)a(t)dt, \\ da(t) = -(i\omega_r + \frac{\kappa}{2})a(t)dt \\ \quad - i \sum_{j=1}^N \Gamma_j \sigma_{-,j}(t)dt - \sqrt{\kappa}dB_{\text{in}}(t), \\ dB_{\text{out}}(t) = \sqrt{\kappa}a(t)dt + dB_{\text{in}}(t), \quad t \geq t_0, \end{cases} \quad (6)$$

which is bilinear.

Remark 3.1: When all atoms are resonant with the resonator, i.e., $\omega_1 = \dots = \omega_N = \omega_r \equiv \omega_s$, rotations $\sigma_{-,j}(t) \rightarrow e^{i\omega_s t}\sigma_{-,j}(t)$, $a(t) \rightarrow e^{i\omega_s t}a(t)$, $B_{\text{in}}(t) \rightarrow e^{i\omega_s t}B_{\text{in}}(t)$, and

$B_{\text{out}}(t) \rightarrow e^{i\omega_s t}B_{\text{out}}(t)$ convert system (6) to

$$\begin{cases} d\sigma_{-,1}(t) = i\Gamma_1\sigma_{z,1}(t)a(t)dt, \\ \vdots \\ d\sigma_{-,N}(t) = i\Gamma_N\sigma_{z,N}(t)a(t)dt, \\ da(t) = -\frac{\kappa}{2}a(t)dt - i \sum_{j=1}^N \Gamma_j \sigma_{-,j}(t)dt - \sqrt{\kappa}dB_{\text{in}}(t), \\ dB_{\text{out}}(t) = \sqrt{\kappa}a(t)dt + dB_{\text{in}}(t), \quad t \geq t_0. \end{cases} \quad (7)$$

In other words, when all the atoms and the cavity are resonant, the frequencies do not affect the system dynamics, except the central frequency of the radiation field.

B. The corresponding linear model

Assume that all the two-level atoms are initially in the ground state and the cavity is in the vacuum state $|0\rangle$. That is, the initial state of the Tavis-Cummings model is

$$|\zeta\rangle = |g_1 g_2 \dots g_N\rangle \otimes |0\rangle. \quad (8)$$

Let

$$X(t) = [\sigma_{-,1}(t) \quad \sigma_{-,2}(t) \quad \dots \quad \sigma_{-,N}(t) \quad a(t)]^\top. \quad (9)$$

Notice that

$$\sigma_{z,j}|\zeta\Phi_0\rangle = -|\zeta\Phi_0\rangle \quad (10)$$

for all $j = 1, \dots, N$. From (6) we get

$$\begin{aligned} dX(t)|\zeta\Phi_0\rangle &= AX(t)|\zeta\Phi_0\rangle dt + BdB_{\text{in}}(t)|\zeta\Phi_0\rangle, \\ dB_{\text{out}}(t)|\zeta\Phi_0\rangle &= CX(t)|\zeta\Phi_0\rangle dt + dB_{\text{in}}(t)|\zeta\Phi_0\rangle, \end{aligned} \quad (11)$$

where

$$A = -i \begin{bmatrix} \omega_1 & 0 & \dots & 0 & \Gamma_1 \\ 0 & \omega_2 & \dots & 0 & \Gamma_2 \\ \vdots & \vdots & \ddots & \vdots & \vdots \\ 0 & 0 & \dots & \omega_N & \Gamma_N \\ \Gamma_1 & \Gamma_2 & \dots & \Gamma_N & \omega_r - \frac{\kappa i}{2} \end{bmatrix}, \quad (12)$$

$$B = [0 \quad 0 \quad \dots \quad 0 \quad -\sqrt{\kappa}]^\top, \quad C = -B^\top.$$

(11) is a linear system. Actually, a linear quantum system of $N + 1$ quantum harmonic oscillators $\bar{a} = [a_1, \dots, a_N, a]^\top$ with system Hamiltonian $H = \omega_r a^* a + \sum_{j=1}^N [\omega_j a_j^* a_j + \Gamma_j (a^* a_j + a_j^* a)]$ and coupling operator $L = \sqrt{\kappa}a$ has the following linear Itô QSDEs

$$\begin{aligned} d\bar{a}(t) &= A\bar{a}(t)dt + BdB_{\text{in}}(t), \\ dB_{\text{out}}(t) &= C\bar{a}(t)dt + dB_{\text{in}}(t), \end{aligned} \quad (13)$$

where A, B, C are exactly those in (12). More discussions on linear quantum systems theory can be found in e.g., [29]–[31]. The transfer function of the linear quantum system (13) is

$$G[s] = 1 + C(sI - A)^{-1}B. \quad (14)$$

Plugging (12) into (14) yields

$$G[s] = \frac{\sum_{k=1}^N \left(\Gamma_k^2 + \frac{1}{N} (s + i\omega_k)(s + i\omega_r - \frac{\kappa}{2}) \right) \prod_{j \neq k}^N (s + i\omega_j)}{\sum_{k=1}^N \left(\Gamma_k^2 + \frac{1}{N} (s + i\omega_k)(s + i\omega_r + \frac{\kappa}{2}) \right) \prod_{j \neq k}^N (s + i\omega_j)}. \quad (15)$$

If $\omega_1 = \dots = \omega_N \equiv \omega_s$, (15) reduces to

$$G[s] = \frac{(\sqrt{N}\bar{\Gamma})^2 + (s + i\omega_s)(s + i\omega_r - \frac{\kappa}{2})}{(\sqrt{N}\bar{\Gamma})^2 + (s + i\omega_s)(s + i\omega_r + \frac{\kappa}{2})}, \quad (16)$$

where $\bar{\Gamma} \triangleq \sqrt{\frac{1}{N} \sum_{k=1}^N \Gamma_k^2}$. Let $\omega_r = \omega_s = 0$, i.e., all atoms are resonant with the cavity resonator. Define $T[s] \triangleq G[s] - 1$. Then

$$|T[i\omega]|^2 = \frac{\kappa^2 \omega^2}{[(\sqrt{N}\bar{\Gamma})^2 - \omega^2]^2 + \frac{\kappa^2}{4} \omega^2}. \quad (17)$$

Clearly, $|T[0]|^2 = 0$ and $|T[i\omega]|^2$ has two peaks attained at $\omega = \pm \sqrt{N}\bar{\Gamma}$, respectively. (If $N = 0$, then $|T[i\omega]|^2$ has only one peak attained at $\omega = 0$, which is the empty cavity case.)

Remark 3.2: Suppose energy enters the system via the input field B_{in} and flows out through the output field B_{out} . $T[s]$ is related to the energy stored in the system. In fact, define the performance variable $z \triangleq C\bar{a}$. Then $T[s]$ is the transfer function from B_{in} to z . It is easy to see that

$$\begin{bmatrix} A + A^\dagger + C^\dagger C & B - C^\dagger \\ B^\dagger - C & 0 \end{bmatrix} = 0. \quad (18)$$

Thus, by the positive real lemma in [33, Theorem 3], the system (13) with the performance variable z is passive. In subsection III-C, we will show that $T[s]$ also reflects the vacuum Rabi mode splitting of the Tavis-Cummings system (6). Hence, $T[s]$ bridges the passivity of the linear quantum system (13) and the vacuum Rabi mode splitting phenomenon exhibited by the Tavis-Cummings system (6).

In the following, we perform structural decomposition on the linear quantum system (13). We partition $\omega_1, \dots, \omega_N$ into M groups according to their degeneracies, where the j th degenerated frequency is denoted by $\tilde{\omega}_j$, ($j = 1, \dots, M$). Let the number of elements be n_j for the group j . In particular, if $M = N$, then $\omega_j \neq \omega_k$ for all $1 \leq j < k \leq N$. For convenience, we can arrange the elements of $\bar{a}(t)$ in (13) so that the matrix A in (12) is of the form

$$\tilde{A} = -i \begin{bmatrix} \tilde{\omega}_1 & \dots & 0 & \dots & 0 & \dots & 0 & \Gamma_{11} \\ \vdots & \ddots & \vdots & \vdots & \vdots & \ddots & \vdots & \vdots \\ 0 & \dots & \tilde{\omega}_1 & \dots & 0 & \dots & 0 & \Gamma_{1n_1} \\ \vdots & \ddots & \vdots & \ddots & \vdots & \ddots & \vdots & \vdots \\ 0 & \dots & 0 & \dots & \tilde{\omega}_M & \dots & 0 & \Gamma_{M1} \\ \vdots & \ddots & \vdots & \ddots & \vdots & \ddots & \vdots & \vdots \\ 0 & \dots & 0 & \dots & 0 & \dots & \tilde{\omega}_M & \Gamma_{Mn_M} \\ \Gamma_{11} & \dots & \Gamma_{1n_1} & \dots & \Gamma_{M1} & \dots & \Gamma_{Mn_M} & \omega_r - \frac{\kappa i}{2} \end{bmatrix}.$$

In other words, we group the elements of $\bar{a}(t)$ according to the partition of the detuned frequencies. It is easy to see that matrices B and C remain the same under this re-arrangement.

Lemma 3.1: Partition $\omega_1, \dots, \omega_N$ into groups as described above. There is an orthogonal matrix \tilde{T} that transforms the linear quantum system (13) with system matrices (\tilde{A}, B, C) to another one, denoted Σ , with system matrices

$$\begin{aligned} \hat{A} &= \tilde{T}^\top \tilde{A} \tilde{T} \\ &= -i \begin{bmatrix} \tilde{\omega}_1 I_{n_1-1} & \mathbf{0} & \dots & \dots & \dots & \mathbf{0} \\ \mathbf{0} & \tilde{\omega}_1 & \dots & \dots & \dots & \sqrt{\tilde{\Gamma}_1} \\ \vdots & \vdots & \ddots & \dots & \dots & \vdots \\ \vdots & \vdots & \vdots & \tilde{\omega}_M I_{n_M-1} & \dots & \mathbf{0} \\ \vdots & \vdots & \vdots & \vdots & \tilde{\omega}_M & \sqrt{\tilde{\Gamma}_M} \\ \mathbf{0} & \sqrt{\tilde{\Gamma}_1} & \dots & \mathbf{0} & \sqrt{\tilde{\Gamma}_M} & \omega_r - \frac{\kappa i}{2} \end{bmatrix}, \\ \hat{B} &= \tilde{T}^\top B = B, \quad \hat{C} = C \tilde{T} = C, \end{aligned} \quad (19)$$

where $\tilde{\Gamma}_j \triangleq \sum_{k=1}^{n_j} \Gamma_{jk}^2$, ($j = 1, \dots, M$).

Proof The proof is constructive. Define a matrix \tilde{T} as

$$\tilde{T} = \begin{bmatrix} \tilde{T}_1 & \mathbf{0} & \dots & \mathbf{0} & \mathbf{0} \\ \mathbf{0} & \tilde{T}_2 & \dots & \mathbf{0} & \mathbf{0} \\ \vdots & \vdots & \ddots & \vdots & \vdots \\ \mathbf{0} & \mathbf{0} & \dots & \tilde{T}_M & \mathbf{0} \\ 0 & 0 & \dots & 0 & 1 \end{bmatrix}, \quad (20)$$

where for each $j = 1, \dots, M$, $\tilde{T}_j = [T_{j1} \ T_{j2} \ \dots \ T_{jn_j}] \in \mathbb{R}^{n_j \times n_j}$, in which

$$\begin{aligned} T_{j1} &= \sqrt{\frac{\Gamma_{j2}^2}{\Gamma_{j1}^2 + \Gamma_{j2}^2}} \begin{bmatrix} -\Gamma_{j1} & 0 & \dots & 0 \end{bmatrix}^\top, \\ T_{j2} &= \sqrt{\frac{\Gamma_{j2}^2 \Gamma_{j3}^2}{(\Gamma_{j1}^2 + \Gamma_{j2}^2)(\Gamma_{j1}^2 + \Gamma_{j2}^2 + \Gamma_{j3}^2)}} \\ &\quad \times \begin{bmatrix} \Gamma_{j1} & 1 & -(\Gamma_{j1}^2 + \Gamma_{j2}^2) & 0 & \dots & 0 \end{bmatrix}^\top, \\ &\vdots \\ T_{j(n_j-1)} &= \sqrt{\frac{\Gamma_{j(n_j-1)}^2 \Gamma_{jn_j}^2}{(\sum_{k=1}^{n_j-1} \Gamma_{jk}^2)(\sum_{k=1}^{n_j} \Gamma_{jk}^2)}} \\ &\quad \times \begin{bmatrix} \Gamma_{j1} & \Gamma_{j2} & \dots & 1 & -\sum_{k=1}^{n_j-1} \Gamma_{jk}^2 & \Gamma_{jn_j}^2 \end{bmatrix}^\top, \\ T_{jn_j} &= \sqrt{\frac{1}{\sum_{k=1}^{n_j} \Gamma_{jk}^2}} \begin{bmatrix} \Gamma_{j1} & \Gamma_{j2} & \dots & \Gamma_{j(n_j-1)} & \Gamma_{jn_j} \end{bmatrix}^\top. \end{aligned}$$

It can be easily verified that \tilde{T} is orthogonal. Moreover, simple algebraic manipulations yield that $\tilde{T}^\top \tilde{A} \tilde{T} = \hat{A}$. \square

The transformed linear quantum system with system matrices (\hat{A}, B, C) has a nice structure. Denote by b_j the system coordinate corresponding to the row whose last entry is $-i\sqrt{\tilde{\Gamma}_j}$ in the matrix \hat{A} , $j = 1, \dots, M$. Then from the

structure of (\hat{A}, B, C) it can be easily seen that this system has a subsystem of the form

$$\left\{ \begin{array}{l} db_1(t) = -i\tilde{\omega}_1 b_1(t)dt - i\sqrt{\Gamma_1}a(t)dt, \\ \vdots \\ db_M(t) = -i\tilde{\omega}_M b_M(t)dt - i\sqrt{\Gamma_M}a(t)dt, \\ da(t) = -(i\omega_r + \frac{\kappa}{2})a(t)dt \\ \quad - i\sum_{j=1}^M \sqrt{\Gamma_j}b_j(t)dt - \sqrt{\kappa}dB_{\text{in}}(t), \\ dB_{\text{out}}(t) = \sqrt{\kappa}a(t)dt + dB_{\text{in}}(t). \end{array} \right. \quad (21)$$

The other $M-1$ subsystems are all isolated systems, which are called decoherence-free subsystems (DFSs) in the linear quantum control literature [29]–[31], [34]. Of course, if $n_j = 1$ for some $j = 1, \dots, M$, there is no such subsystem as can be seen clearly from the matrix \hat{A} in (19). According to quantum linear systems theory, the subsystem (21) is a controllable and observable subsystem.

The following result is an immediate consequence of Lemma 3.1.

Corollary 3.1: If $\omega_1 = \dots = \omega_N \equiv \omega_s$, then $M = 1$ and $n_1 = N$ in (19). Accordingly, the transformation matrix \tilde{T} in (20) reduces to

$$\left[\begin{array}{c|c} \tilde{T}_1 & \mathbf{0} \\ \hline 0 & 1 \end{array} \right] \equiv T, \quad (22)$$

which transforms the quantum linear system (13) to a new one with system matrices

$$\begin{aligned} \hat{A} &= T^\top A T = \left[\begin{array}{c|c} \hat{A}_{\bar{c}\bar{o}} & \mathbf{0} \\ \hline \mathbf{0} & \hat{A}_{co} \end{array} \right], \\ \hat{B} &= T^\top B = \left[\begin{array}{c} \hat{B}_{\bar{c}\bar{o}} \\ \hat{B}_{co} \end{array} \right], \hat{C} = C T = [\hat{C}_{\bar{c}\bar{o}} \mid \hat{C}_{co}], \end{aligned} \quad (23)$$

where

$$\begin{aligned} \hat{A}_{\bar{c}\bar{o}} &= -i\omega_s I_{N-1}, \quad \hat{A}_{co} = - \left[\begin{array}{cc} i\omega_s & i\sqrt{N\Gamma} \\ i\sqrt{N\Gamma} & i\omega_r + \frac{\kappa}{2} \end{array} \right] \\ \hat{B}_{\bar{c}\bar{o}} &= \mathbf{0}, \quad \hat{B}_{co} = - \left[\begin{array}{c} 0 \\ \sqrt{\kappa} \end{array} \right], \hat{C}_{\bar{c}\bar{o}} = \mathbf{0}, \quad \hat{C}_{co} = [0 \quad \sqrt{\kappa}]. \end{aligned} \quad (24)$$

Remark 3.3: In the linear quantum systems theory [29]–[31], [34] DFSs are defined in the Heisenberg picture. On the other hand, decoherence-free subspaces widely used in the quantum information community are characterized by density matrices in the Schrödinger picture; see references 3–8 in [35]. It can be seen that the eigenvectors $\{T_1, \dots, T_{N-1}\}$ of the DFS with system matrices $(\hat{A}_{\bar{c}\bar{o}}, \hat{B}_{\bar{c}\bar{o}}, \hat{C}_{\bar{c}\bar{o}})$ constitute a basis of the decoherence-free subspace. Some examples will be given in subsection III-C.

Remark 3.4: The coupling operator $L = \sqrt{\kappa}a$ is called the noise operator in [35], through which the system information leaks irreversibly into its surrounding environment. It can be clearly seen from (23)–(24) that L has no effect on the DFS with system matrices $(\hat{A}_{\bar{c}\bar{o}}, \hat{B}_{\bar{c}\bar{o}}, \hat{C}_{\bar{c}\bar{o}})$, thus the DFS is robust with respect to the cavity decay rate κ . This is the so-called γ -robustness in [35, Definition 3]. Moreover, from (24) it can

be seen that the DFS is robust with respect to the variations of the atom-cavity coupling strengths Γ_j as well. Finally, the DFS is not attractive from [35, Proposition 3], which is for noiseless subsystems and reduces to DFSs when $\mathcal{H}_F \simeq \mathbb{C}$; see [35, Definition 8 and subsection II-A] for details.

C. Physical interpretation

The discussions of the Tavis-Cummings model in the previous subsection in terms of linear quantum systems theory appear purely mathematical; however, these results can indeed reveal several typical features of the Tavis-Cummings model.

Firstly, from (16), it can be seen that the collection of the N atoms act as a giant atom of detuned frequency ω_s and coupling strength $\sqrt{N\Gamma}$, which reflects the \sqrt{N} -scaling of the collective coupling strength; in other words, this giant atom decays N times as fast as a single atom. This is the physical basis of superradiance.

Secondly, the two peaks of the transfer function $|T[i\omega]|^2$ in (17) at $\omega = \pm\sqrt{N\Gamma}$ echo the vacuum Rabi mode splitting in the Tavis-Cummings model, see, e.g., [4, Fig. 2(b)], [5, Fig. 3], and [6, Fig. 2(b)].

Thirdly, the controllable and observable subsystem echos the bright states and the uncontrollable and unobservable subsystems echo the dark states of the Tavis-Cummings model. For simplicity, we look at the simplest case of $\omega_1 = \dots = \omega_N \equiv \omega_s$. In this case, according to Corollary 3.1, there is an orthogonal matrix T which yields a system with system matrices given in (23). Let $N = 3$ and assume the coupling constants $\Gamma_1 = -\Gamma_2 = \Gamma_3$. (In [5], $\Gamma_1, \Gamma_2, \Gamma_3$ are respectively g_A, g_B, g_C . As shown in [5, Table 1], the actual values of $\Gamma_1, -\Gamma_2, \Gamma_3$ are not exactly identical, but the discrepancy has negligible effect as can be seen from consistency between the red region (for real data) and the white dashed curves (for theoretical calculation) in [5, Fig. 3].) The orthogonal transformation matrix T can be calculated as $T_1 = \frac{1}{\sqrt{2}} [1 \ 1 \ 0 \ 0]^\top$, $T_2 = \frac{1}{\sqrt{6}} [-1 \ 1 \ 2 \ 0]^\top$, $T_3 = \frac{1}{\sqrt{3}} [1 \ -1 \ 1 \ 0]^\top$, and $T_4 = [0 \ 0 \ 0 \ 1]^\top$. Identify g with 0 and e with 1 respectively. It can be verified that the dark states $|3, 1d_1\rangle = \frac{1}{\sqrt{2}}(|e, g, g, 0\rangle - |g, g, e, 0\rangle)$ and $|3, 1d_2\rangle = \frac{1}{\sqrt{2}}(|g, e, g, 0\rangle + |g, g, e, 0\rangle)$ in [5] can be expressed as $|3, 1d_1\rangle = \frac{1}{2}T_1 - \frac{\sqrt{3}}{2}T_2$, and $|3, 1d_2\rangle = \frac{1}{2}T_1 + \frac{\sqrt{3}}{2}T_2$ respectively, while the bright states $|3, 1\pm\rangle = \frac{1}{\sqrt{2}}|g, g, g, 1\rangle \pm \frac{1}{\sqrt{6}}|e, g, g, 0\rangle$ in [5] can be written as $|3, 1\pm\rangle = \frac{1}{\sqrt{2}}(T_4 \pm T_3)$. In other words, the dark states $|3, 1d_1\rangle$ and $|3, 1d_2\rangle$ live in the decoherence-free subspace spanned by T_1 and T_2 , while the bright states $|3, 1\pm\rangle$ live in the controllable and observable subspace spanned by T_3 and T_4 .

Take the case $N = 2$ for another example. Similar correspondence can be found between the eigenstates of the Tavis-Cummings model (6) and the vectors in (22). Regard the states $|g, e, 0\rangle$, $|e, g, 0\rangle$, $|g, g, 1\rangle$ in [9] as vectors $[0 \ 1 \ 0]^\top$, $[1 \ 0 \ 0]^\top$, and $[0 \ 0 \ 1]^\top$, respectively. In the resonant ($\omega_r = \omega_s$) case, the dark state $|0\rangle_{r3} = \frac{1}{\sqrt{N\Gamma}}(\Gamma_1|g, e, 0\rangle - \Gamma_2|e, g, 0\rangle)$ in [9, Appendix C-3] is $-T_1$, and the two bright states $|\pm\rangle_{r3} = \frac{1}{N\Gamma}(\Gamma_2|g, e, 0\rangle + \Gamma_1|e, g, 0\rangle \pm \sqrt{N\Gamma}|g, g, 1\rangle)$ in [9, Appendix C-3] are $\frac{1}{\sqrt{2}}(T_2 \pm T_3)$. Also, $|0\rangle_{r3}$ and $|\pm\rangle_{r3}$ are respectively

$-|2, 1d\rangle$ and $-|2, 1\pm\rangle$ in [5] when $\Gamma_1 = -\Gamma_2 = \Gamma_3$. Moreover, in the dispersive regime ($\Delta_r = |\omega_r - \omega_s| \gg \Gamma_j$, $j = 1, \dots, N$) considered in [9, Appendix C], the three states $|+\rangle_{r3}, |-\rangle_{r3}, |1'\rangle_{r3}$ given in [9, (C18)] can be expressed by $|+\rangle_{r3} = -T_1$, $|-\rangle_{r3} = \frac{1}{\sqrt{N\Gamma^2 + \Delta_r^2}}(\Delta_r T_2 - \sqrt{N\Gamma} T_3) \approx T_2$, and $|1'\rangle_{r3} = \frac{1}{\sqrt{N\Gamma^2 + \Delta_r^2}}(\sqrt{N\Gamma} T_2 + \Delta_r T_3) \approx T_3$. Thus, in both cases, the dark states live in the space spanned by T_1 while the bright states live in the space spanned by T_2 and T_3 .

Fourthly, the dynamics of two remote spin ensembles coupled by a cavity bus are experimentally studied in [7]. The Hamiltonian of the system is given in [7, (2)], which is of the form of H_{TC} for the Tavis-Cummings model. When $\varphi \approx 48.1^\circ$ in [7, Fig. 2(b)], both spin ensembles resonate with the cavity mode. Thus, this particularly interesting case can be analyzed by Corollary 3.1. Indeed, the eigenstates $|\pm\rangle$ in [7, (3)] and the dark mode $|D\rangle$ in [7, (4)] can be obtained by means of the orthonormal matrix T in Corollary 3.1.

Fifthly, in subsections IV-A and IV-B we study how the Tavis-Cummings model (6) responds to a continuous-mode single-photon input state, where the linear model developed in subsection III-B plays an essential role.

Finally, the single-excitation superradiant and subradiant states of the Tavis-Cummings model can be analyzed by means of the quantum linear systems theory presented in subsection III-B; see Remark 4.2 in subsection IV-C.

IV. THE SINGLE-EXCITATION CASE

In this section, we investigate the dynamics of the Tavis-Cummings model when there is only one excitation.

A. Response to single-photon inputs

In this subsection, we derive an analytic expression of the steady-state output field state when the Tavis-Cummings model is initialized in the state $|\zeta\rangle$ given in (8), and driven by a single-photon state.

We start with the following lemma which discusses the controllability ([34, Sec. III-B], [29, Definition 1]) of the passive linear quantum system (13).

Lemma 4.1: The passive linear quantum system (13) is controllable if and only if $\omega_j \neq \omega_k$ for all $1 \leq j < k \leq N$.

Proof Let a scalar $\lambda \in \mathbb{C}$ and a vector $x = [x_1, \dots, x_{N+1}]^\top \in \mathbb{C}^{N+1}$ satisfy

$$Ax = \lambda x, \quad x^\dagger B = 0. \quad (25)$$

We have

$$x_{N+1} = 0, \quad -i\omega_k x_k = \lambda x_k, \quad k = 1, \dots, N, \quad (26)$$

and

$$\sum_{k=1}^N \Gamma_k x_k = 0. \quad (27)$$

Necessity. We prove it by contradiction. Without loss of generality, assume $\omega_1 = \omega_2$. We choose $\lambda = -i\omega_1$, $x_1 = \Gamma_2$, $x_2 = -\Gamma_1$, and $x_j = 0$ for all $j = 3, \dots, N+1$. Clearly, the scalar λ and the *nonzero* vector x satisfy (25). This means that the system is not controllable. A contradiction is reached.

Sufficiency. If $x_j \neq 0$ for some $j = 1, \dots, N$, then by (26) $\lambda = -i\omega_j$. As $\omega_j \neq \omega_k$ for all $1 \leq j < k \leq N$, again by (26) $x_k = 0$ for all $j \neq k$. Thus, (27) reduces to $\Gamma_j x_j = 0$, which yields $x_j = 0$. This shows that any vector x satisfying (25) must be a zero vector. Hence, the system is controllable. \square

For system (21), $\tilde{\omega}_j \neq \tilde{\omega}_k$ for all $1 \leq j < k \leq M$. By Lemma 4.1, system (21) is Hurwitz stable.

With the aid of Lemma 4.1, the main result of this section can be derived.

Theorem 4.1: Assume that the Tavis-Cummings model (6) is initialized in the state $|\zeta\rangle = |g_1 g_2 \dots g_N\rangle \otimes |0\rangle$ and driven by a single-photon input state with pulse shape ξ . The steady-state ($t \rightarrow \infty$ and $t_0 \rightarrow -\infty$) output field state is a single-photon state with the frequency-domain pulse shape

$$\eta[i\omega] = G[i\omega]\xi[i\omega], \quad (28)$$

where the transfer function $G[s]$ is given by (15).

Proof By system (6) and (10), we have

$$\begin{aligned} \langle \zeta \Phi_0 | b_{\text{out}}(t) &= C e^{A(t-t_0)} \langle \zeta \Phi_0 | X(t_0) \\ &+ \int_{t_0}^t C e^{A(t-\tau)} \langle \zeta \Phi_0 | b_{\text{in}}(\tau) d\tau + \langle \zeta \Phi_0 | b(t). \end{aligned}$$

If A is Hurwitz stable, then $C e^{A(t-t_0)} \langle \zeta \Phi_0 | X(t_0) \rightarrow 0$ as $t_0 \rightarrow -\infty$. If A is not Hurwitz stable, then by Corollary 3.1, the $\bar{c}\bar{o}$ subsystem does not affect the input-output behavior, while the $c\bar{o}$ subsystem is Hurwitz stable; see Proposition 7.1 in the Appendix. Hence we also have $C e^{A(t-t_0)} \langle \zeta \Phi_0 | X(t_0) \rightarrow 0$ as $t_0 \rightarrow -\infty$. As a result, sending $t_0 \rightarrow -\infty$, we get

$$\langle \zeta \Phi_0 | b_{\text{out}}(t) = \int_{-\infty}^{\infty} g_G(t-r) \langle \zeta \Phi_0 | b_{\text{in}}(r) dr, \quad (29)$$

where $g_G(t)$ is the impulse response function associated to the transfer function $G[s]$ in (14). As $b_{\text{out}}(t) = U^* b(t, t_0)_{\text{in}}(t) U(t, t_0)$, we have

$$\langle \zeta \Phi_0 | b_{\text{in}}(t) = \int_{-\infty}^{\infty} g_G(t-r) \langle \zeta \Phi_0 | b^-(r, -\infty) dr, \quad (30)$$

where $b^-(t, t_0) \triangleq U(t, t_0) b_{\text{in}}(t) U^*(t, t_0)$. Then following the stable inverse technique in [24, Lemma 1], we can get

$$\begin{aligned} b^{*-}(r, -\infty) | \zeta \Phi_0 \rangle &= \int_{-\infty}^{\infty} g_G^*(r-t) b_{\text{in}}^*(t) dt | \zeta \Phi_0 \rangle \\ &= \int_{-\infty}^{\infty} g_G(t-r) b_{\text{in}}^*(t) dt | \zeta \Phi_0 \rangle, \end{aligned} \quad (31)$$

and thus

$$\int_{-\infty}^{\infty} \xi(r) b^{*-}(r, -\infty) | \zeta \Phi_0 \rangle dr = \int_{-\infty}^{\infty} \eta(t) b_{\text{in}}^*(t) | \zeta \Phi_0 \rangle dt, \quad (32)$$

where $\eta(t)$ is the time-domain counterpart of $\eta[i\omega]$ in (28). Consequently, the steady-state joint system-field state in [24, Eq. (85)] is

$$\rho_\infty = |\zeta\rangle \langle \zeta| \otimes |1_\eta\rangle \langle 1_\eta|. \quad (33)$$

The steady-state output field state ρ_{out} is then obtained by tracing over the initial system state, i.e., $\rho_{\text{out}} = \text{Tr}_{\text{sys}}[\rho_\infty] = |1_\eta\rangle \langle 1_\eta|$, which is a pure state $|1_\eta\rangle$. \square

B. Simulation results for $N \leq 4$

In this subsection, we illustrate Theorem 4.1 by a special case of $N \leq 4$, i.e., at most four two-level atoms are coupled to the cavity. The single-photon input state is supposed to have a rising exponential pulse shape

$$\xi(t) = \begin{cases} \sqrt{\gamma}e^{\frac{\gamma}{2}t}, & t \leq 0, \\ 0, & t > 0, \end{cases} \quad (34)$$

where γ denotes the full width at half maximum (FWHM) of the Lorentzian spectrum. The input and output photon probability distributions are shown in Fig. 2. It is worthwhile to notice that the carrier frequency of the single-photon input field is not shown in (34), the reason is that all the frequencies in the system Hamiltonian H_{TC} in (5) are detuned from this carrier frequency.

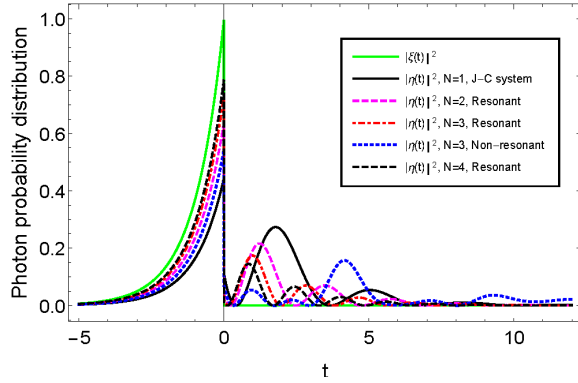


Fig. 2. The input and output photon probability distributions. The input photon probability distribution is plotted as the green curve; the red dot dashed curve plots the output photon probability distribution in the case that all the three two-level atoms are resonant with each other ($\omega_1 = \omega_2 = \omega_3 = 0$); the non-resonant case is plotted as the blue dotted curve ($\omega_1 = 1, \omega_2 = -1, \omega_3 = 0$); the output photon probability distributions for the resonant cases of $N = 1$ (Jaynes-Cummings system), $N = 2$ and $N = 4$ are shown as the black solid, magenta dashed, and black dashed curves respectively. ($\gamma = \kappa = 1, \omega_r = 0$, and $\Gamma_j = 1, j = 1, \dots, 4$.)

In Fig. 2, it can be observed that the emitted photon is more likely to be found when $t < 0$ as the number of atoms increases, which means it interacts with the Jaynes-Cummings system (the $N = 1$ case) more easily than with the Tavis-Cummings model. On the other hand, the Rabi oscillation at $t > 0$ indicates that the photon can be repeatedly absorbed and emitted by the two-level atoms. The oscillation also becomes stronger when there are more atoms, which indicates that the added atoms increase the time for the photon to escape from the cavity. The Rabi oscillation monotonically decays when all the atoms are resonant with each other, while revivals can be observed in the non-resonant case (the blue dotted curve). Moreover, oscillation sustains much longer in the non-resonant case than in the resonant case. Finally, simulation shows that in the resonant case, the shapes of the input and output pulses are quite close to each other when N is large, showing that the input single photon hardly interacts with the atomic ensemble. This phenomenon is confirmed by $\lim_{N \rightarrow \infty} G[i\omega] = 1$ for any fixed ω , where $G[s]$ is given in (16).

C. An analytic form of the superposition state

In this subsection, an analytic form of the joint system-field state is derived.

The following theorem is the main result of this subsection.

Theorem 4.2: Assume that the N two-level atoms of the Tavis-Cummings model are resonant with each other, i.e., $\omega_1 = \dots = \omega_N \equiv \omega_s$, the k th two-level atom is in the excited state, the others are in the ground state, the cavity is empty and the Tavis-Cummings model is driven by the vacuum input state. That is, the initial joint system-field state is $|\Psi_k(0)\rangle = |g_1 g_2 \dots e_k \dots g_N 0\rangle \otimes |\Phi_0\rangle$. Then the joint system-field state is

$$\begin{aligned} |\Psi_k(t)\rangle = & c_k(t) |g_1 g_2 \dots e_k \dots g_N 0 \Phi_0\rangle \\ & + \sum_{j \neq k}^N c_j(t) |g_1 g_2 \dots e_j \dots g_N 0 \Phi_0\rangle \\ & + c_{N+1,k}(t) \int_0^t \varphi(\tau) dB_{in}^*(\tau) |g_1 g_2 \dots g_N 0 \Phi_0\rangle \\ & + c_{N+2,k}(t) |g_1 g_2 \dots g_N 1 \Phi_0\rangle, \end{aligned} \quad (35)$$

where

$$\begin{aligned} c_k(t) &= \frac{e^{\frac{N-2}{2}i\omega_s t}}{2\chi N\Gamma^2} \left[2\chi \sum_{j \neq k}^N \Gamma_j^2 + \Gamma_k^2 \left(\lambda_1 e^{-\frac{\lambda_2 t}{4}} - \lambda_2 e^{-\frac{\lambda_1 t}{4}} \right) \right], \\ c_j(t) &= \frac{-\Gamma_j \Gamma_k e^{\frac{N-2}{2}i\omega_s t}}{2\chi N\Gamma^2} \left[2\chi - \left(\lambda_1 e^{-\frac{\lambda_2 t}{4}} - \lambda_2 e^{-\frac{\lambda_1 t}{4}} \right) \right], j \neq k, \\ c_{N+1,k}(t) &= \frac{\Gamma_k}{\sqrt{N}\Gamma} e^{\frac{N-2}{2}i\omega_s t}, \\ c_{N+2,k}(t) &= \frac{-4i\Gamma_k \sinh(\frac{1}{4}\chi t)}{\chi} e^{-\frac{1}{4}[\kappa + 2i(\omega_r - (N-1)\omega_s)]t}, \\ \varphi(\tau) &= \frac{-4i\Gamma \sqrt{\kappa N} \sinh(\frac{1}{4}\chi \tau)}{\chi} e^{-\frac{\kappa \tau + 2i[\omega_s(\tau-t) + \omega_r \tau - \omega_s t]}{4}}, \end{aligned} \quad (36)$$

with $\lambda_1 = \kappa + \chi + 2i(\omega_r - \omega_s)$, $\lambda_2 = \kappa - \chi + 2i(\omega_r - \omega_s)$, and $\chi = \sqrt{(\kappa + 2i\omega_r - 2i\omega_s)^2 - 16N\Gamma^2}$. Moreover, in the steady state ($t = \infty$), by ignoring the rotating term $e^{\frac{N-2}{2}i\omega_s t}$ in the coefficients in (36) (equivalently, setting $\omega_s = 0$) the superposition state (35) becomes

$$\begin{aligned} |\Psi_k(\infty)\rangle = & c_k(\infty) |g_1 g_2 \dots e_k \dots g_N 0 \Phi_0\rangle \\ & + \sum_{j \neq k}^N c_j(\infty) |g_1 g_2 \dots e_j \dots g_N 0 \Phi_0\rangle \\ & + c_{N+1,k}(\infty) |g_1 g_2 \dots g_N 0 1 \varphi\rangle, \end{aligned} \quad (37)$$

where

$$\begin{aligned} c_k(\infty) &= \frac{1}{N\Gamma^2} \sum_{j \neq k}^N \Gamma_j^2, \quad c_j(\infty) = \frac{-\Gamma_j \Gamma_k}{N\Gamma^2}, j \neq k, \\ c_{N+1,k}(\infty) &= \frac{\Gamma_k}{\sqrt{N}\Gamma}. \end{aligned} \quad (38)$$

The proof of Theorem 4.2 follows the recursive formula for joint system-field states of general quantum systems; see Remark 6.3 in Section VI.

Remark 4.1: By Theorem 4.2, it can be seen that the cavity is eventually empty ($c_{N+2,k}(\infty) = 0$), which results in a superposition state of the two-level atoms and the output field. Moreover, by (38), the steady-state excitation probabilities of two-level atoms are independent of the cavity resonant frequency ω_r , as well as the atomic transition frequency ω_s .

It is well-known in quantum optics that the collective radiation of an ensemble of two-level atoms can be accelerated by superradiance or inhibited by subradiance [1], [2], [6], the following corollary gives the steady state of the Tavis-Cummings model initialized in a superposition state of the superradiant and subradiant states.

Corollary 4.1: Assume that the N two-level atoms in the Tavis-Cummings model are resonant with each other, i.e., $\omega_1 = \dots = \omega_N \equiv \omega_s$. Let the system be driven by the vacuum input state and initialized in the following superposition state $(\alpha|B_N\rangle + \beta|D_N\rangle) \otimes |0\rangle$, where $|\alpha|^2 + |\beta|^2 = 1$, and the single-excitation superradiant state $|B_N\rangle$ and subradiant state $|D_N\rangle$ are respectively

$$\begin{aligned} |B_N\rangle &= \frac{1}{\sqrt{N}} \sum_{k=1}^N |g_1 \dots e_k \dots g_N\rangle, \\ |D_N\rangle &= \frac{1}{\sqrt{N}} \sum_{k=1}^N e^{-i\phi_k} |g_1 \dots e_k \dots g_N\rangle \end{aligned} \quad (39)$$

with $\phi_k = \frac{2\pi}{N}k$. Then the joint system-field state is

$$|\Psi'(t)\rangle = \frac{1}{\sqrt{N}} \sum_{k=1}^N (\alpha + \beta e^{-i\phi_k}) |\Psi_k(t)\rangle, \quad (40)$$

where $|\Psi_k(t)\rangle$ is given in (35). Moreover, in the steady state ($t = \infty$), by ignoring the rotating term $e^{\frac{N-2}{2}i\omega_s t}$ in the coefficients in (36) (equivalently, setting $\omega_s = 0$), the superposition state (40) becomes

$$|\Psi'(\infty)\rangle = \frac{1}{\sqrt{N}} \sum_{k=1}^N (\alpha + \beta e^{-i\phi_k}) |\Psi_k(\infty)\rangle, \quad (41)$$

where $|\Psi_k(\infty)\rangle$ is given in (37).

The proof of Corollary 4.1 is omitted.

Let $\alpha = 0$, $\beta = 1$, i.e., the Tavis-Cummings model is initialized in the pure state $|D_N 0\rangle$. By Corollary 4.1, the joint system-field steady state is

$$|\Psi'(\infty)\rangle = \frac{1}{\sqrt{N}} \sum_{k=1}^N c'_k(\infty) |g_1 \dots e_k \dots g_N 0 \Phi_0\rangle, \quad (42)$$

where

$$c'_k(\infty) = \frac{e^{-i\phi_k} \sum_{j \neq k}^N \Gamma_j^2 - \Gamma_k \sum_{j \neq k}^N e^{-i\phi_j} \Gamma_j}{N\Gamma^2}, \quad (43)$$

provided that $\omega_s = 0$. Assume further that the atoms are all equally coupled with the cavity, i.e., $\Gamma_1 = \Gamma_2 = \dots = \Gamma_N$, then the steady state (42) reduces to

$$|\Psi'(\infty)\rangle = |D_N 0\rangle \otimes |\Phi_0\rangle. \quad (44)$$

In other words, in the steady state, the single excitation only exists in the two-level atoms which have the same excitation probability $\frac{1}{N}$. The Tavis-Cummings system cannot emit a

photon into the cavity or the output field. This theoretical result is consistent with the experimental results given in [6, Fig. 2(c), Fig. 4(a)], where small fluctuations of the collective swapping dynamics are due to the inhomogeneity of the coupling strengths. In fact, when $\Gamma_1 = \Gamma_2 = \dots = \Gamma_N$ and $\omega_s = 0$, by Corollary 3.1, $\hat{A}_{\bar{c}0} = 0$, and thus the subsystem $(\hat{A}_{\bar{c}0}, \hat{B}_{\bar{c}0}, \hat{C}_{\bar{c}0})$ is static. On the other hand, it is easy to show that $|\Psi(t)\rangle \equiv |\Psi(0)\rangle = |D_N 0\rangle \otimes |\Phi_0\rangle$ for all $t \geq 0$.

Let $\alpha = 1$, $\beta = 0$, i.e., the Tavis-Cummings model is initialized in the pure state $|B_N 0\rangle$. In this case, the steady state is

$$\begin{aligned} |\Psi'(\infty)\rangle &= \frac{1}{\sqrt{N}} \sum_{k=1}^N \left(c'_k(\infty) |g_1 \dots e_k \dots g_N 0 \Phi_0\rangle \right. \\ &\quad \left. + c_{N+1,k}(\infty) |g_1 g_2 \dots g_N 0 1 \varphi\rangle \right), \end{aligned} \quad (45)$$

where the pulse shape φ is given in (36), and $c'_k(\infty) = \frac{\sum_{j \neq k}^N \Gamma_j^2 - \Gamma_k \sum_{j \neq k}^N \Gamma_j}{N\Gamma^2}$, provided that $\omega_s = 0$, and $c_{N+1,k}(\infty)$ is given in (38). Assume further that the atoms are all equally coupled with the cavity, i.e., $\Gamma_1 = \Gamma_2 = \dots = \Gamma_N$, the steady state (45) reduces to

$$|\Psi'(\infty)\rangle = |g_1 g_2 \dots g_N 0 1 \varphi\rangle. \quad (46)$$

In other words, due to the existence of cavity decay rate κ , the Tavis-Cummings system eventually emits a photon into the field.

Remark 4.2: The superradiant state $|B_N\rangle$ and subradiant state $|D_N\rangle$ can be represented by the eigenvectors given in (22), respectively. For simplicity, we assume the coupling strengths $\Gamma_1 = \dots = \Gamma_N \equiv \Gamma$. If the state $|g_1 \dots e_k \dots g_N 0\rangle$ is viewed as a column vector $[0 \dots 1 \dots 0]^T$ (the k th element is 1 and the others are 0), then $|B_N 0\rangle$ is exactly the vector T_N in (22). Moreover, $A|B_N 0\rangle = -i\omega_s T_N - i\sqrt{N}\Gamma T_{N+1}$, which lives in the linear span of the two vectors T_N and T_{N+1} of the controllable/observable subsystem \hat{A}_{co} given in (24). Hence, the single excitation swaps among all the two-level atoms and the cavity. This echoes the collective swapping dynamics shown in [6, Fig. 2(a)]. Moreover, as shown in (46), eventually all the oscillations will die out as the photon is emitted into the external field due to the lossy nature of the cavity. On the other hand, the subradiant state $|D_N 0\rangle$ can be represented by

$$|D_N 0\rangle = \sum_{j=1}^{N-1} \alpha_j T_j, \quad (47)$$

where $\alpha_j = -\sqrt{\frac{j+1}{jN}} \left[e^{-i\phi_{j+1}} + \frac{1}{j+1} \sum_{k=j+2}^N e^{-i\phi_k} \right]$, for $j = 1, 2, \dots, N-2$, and $\alpha_{N-1} = -\frac{1}{\sqrt{N-1}} e^{-i\phi_N}$. Therefore, the subradiant state given in (47) is a linear combination of the $N-1$ eigenvectors of the DFS given in (24). In this case, the Tavis-Cummings model is neither reachable by its input nor detectable by its output. Thus, the two-level atoms are decoupled from the cavity mode and the external field, and the Tavis-Cummings model initialized in $|D_N 0\rangle$ cannot emit a photon into the cavity or even the external field, and remains in the subradiant state (44).

V. THE MULTI-EXCITATION CASE

In Section IV, we studied the single-excitation dynamics of the Tavis-Cummings model. In this section, we present numerical studies of the multi-excitation scenario. For ease of representation, we calculate the excitation probabilities of the *first* two-level atom.

A. The reduced density matrix of the first two-level atom

In this subsection, we present the master equation for the Tavis-Cummings model; we also give the expression of the reduced density of the first two-level atom.

According to [23], the master equation of the Tavis-Cummings model driven by a single-photon input $|1_\xi\rangle$ is

$$\begin{aligned}\dot{\bar{\rho}}^{11}(t) &= \mathcal{L}^* \bar{\rho}^{11}(t) + \xi(t)[\bar{\rho}^{01}(t), L^*] + \xi^*(t)[L, \bar{\rho}^{10}(t)], \\ \dot{\bar{\rho}}^{10}(t) &= \mathcal{L}^* \bar{\rho}^{10}(t) + \xi(t)[\bar{\rho}^{00}(t), L^*], \\ \dot{\bar{\rho}}^{01}(t) &= \mathcal{L}^* \bar{\rho}^{01}(t) + \xi^*(t)[L, \bar{\rho}^{00}(t)], \\ \dot{\bar{\rho}}^{00}(t) &= \mathcal{L}^* \bar{\rho}^{00}(t), \quad t \geq t_0,\end{aligned}\quad (48)$$

where the initial states are

$$\bar{\rho}^{11}(t_0) = \bar{\rho}^{00}(t_0) = |\zeta\rangle\langle\zeta|, \quad \bar{\rho}^{10}(t_0) = \bar{\rho}^{01}(t_0) = 0 \quad (49)$$

with $|\zeta\rangle$ being the initial system state. As we will focus on the excitation probability of the first two-level atom, we use the partial trace to get its reduced density operator

$$\begin{aligned}\rho_{A_1}(t) &\triangleq \text{Tr}_{A_N}[\cdots \text{Tr}_{A_2}[\text{Tr}_{\text{cav}}[\bar{\rho}^{11}(t)]]] \\ &= \sum \langle z_2 z_3 \dots z_N n | \bar{\rho}^{11}(t) | z_2 z_3 \dots z_N n \rangle,\end{aligned}\quad (50)$$

where $|z_j\rangle = |g_j\rangle$ or $|e_j\rangle$, $j = 2, 3, \dots, N$, and $|n\rangle$ is the state of the cavity.

Remark 5.1: When the input is in the vacuum state $|\Phi_0\rangle$, (48)-(49) reduce to the commonly used master equation

$$\dot{\bar{\rho}}^{00}(t) = \mathcal{L}^* \bar{\rho}^{00}(t), \quad \bar{\rho}^{00}(t_0) = |\zeta\rangle\langle\zeta|, \quad t \geq t_0. \quad (51)$$

Accordingly, the excitation probability of the first two-level atom is given by $\langle e_1 | \rho_{A_1}(t) | e_1 \rangle$, where $\rho_{A_1}(t)$ should be computed via (50) by replacing $\bar{\rho}^{11}(t)$ with $\bar{\rho}^{00}(t)$.

In the following simulations, we assume that there are three resonant two-level atoms that are equally coupled to the cavity, i.e., $\omega_1 = \omega_2 = \omega_3 = \omega_r = 1$ and $\Gamma_1 = \Gamma_2 = \Gamma_3 = 1$. Also let $\kappa = 1.5$. When the input field is in the single photon state $|\Phi_1\rangle$, we use a Gaussian pulse shape

$$\xi(t) = \left(\frac{\Omega^2}{2\pi}\right)^{1/4} \exp\left[-\frac{\Omega^2}{4}(t - t_p)^2\right], \quad (52)$$

where t_p is the peak arrival time of the photon, and Ω is the frequency bandwidth. Set $t_p = 3$ and $\Omega = 2\kappa$. See the green solid curve in Fig. 3 for the plot of $|\xi(t)|^2$. As $|\xi(t)|^2 \approx 0$ when $t = 0$, it is safe to let the initial time t_0 be 0.

B. One initially excited atom plus a single-photon input

Assume that one of the two-level atoms is in the excited state, the cavity is empty, and the system is driven by a single-photon input. Then there are two excitations in the whole system. According to the reduced density matrix (50), the

excitation probability of the first two-level atom in this two-excitation case can be calculated as

$$\begin{aligned}P_{\text{TLS1}}(t) &= \langle e_1 | \rho_{A_1}(t) | e_1 \rangle \\ &= \langle e_1 g_2 g_3 0 | \bar{\rho}^{11}(t) | e_1 g_2 g_3 0 \rangle + \langle e_1 e_2 g_3 0 | \bar{\rho}^{11}(t) | e_1 e_2 g_3 0 \rangle \\ &\quad + \langle e_1 g_2 e_3 0 | \bar{\rho}^{11}(t) | e_1 g_2 e_3 0 \rangle + \langle e_1 g_2 g_3 1 | \bar{\rho}^{11}(t) | e_1 g_2 g_3 1 \rangle,\end{aligned}$$

where the term $\langle e_1 g_2 g_3 0 | \bar{\rho}^{11}(t) | e_1 g_2 g_3 0 \rangle$ indicates that a photon is in the external field.

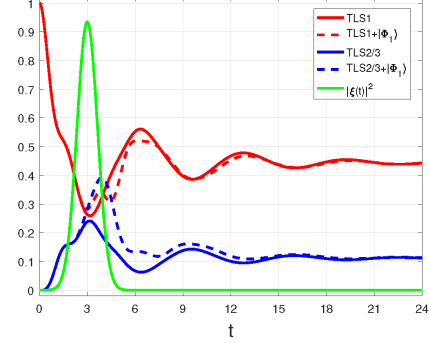


Fig. 3. The excitation probabilities of the first two-level atom. Green solid curve: $|\xi(t)|^2$; red solid curve (TLS1: $|e_1 g_2 g_3 0\rangle \otimes |\Phi_0\rangle$); blue solid curve (TLS2/3: $|g_1 e_2 g_3 0\rangle \otimes |\Phi_0\rangle$ or $|g_1 g_2 e_3 0\rangle \otimes |\Phi_0\rangle$); red dashed curve (TLS1+ $|\Phi_1\rangle$: $|e_1 g_2 g_3 0\rangle \otimes |\Phi_1\rangle$); blue dashed curve (TLS2/3+ $|\Phi_1\rangle$: $|g_1 e_2 g_3 0\rangle \otimes |\Phi_1\rangle$ or $|g_1 g_2 e_3 0\rangle \otimes |\Phi_1\rangle$).

We consider the effect of single-photon input state on the excitation probability, which is simulated in Fig. 3. The red solid curve is for the case when the initial joint system-field state $|\Psi(0)\rangle = |e_1 g_2 g_3 0\rangle \otimes |\Phi_0\rangle$, the blue solid curve is for $|\Psi(0)\rangle = |g_1 e_2 g_3 0\rangle \otimes |\Phi_0\rangle$ or $|\Psi(0)\rangle = |g_1 g_2 e_3 0\rangle \otimes |\Phi_0\rangle$, the red dashed curve is for $|\Psi(0)\rangle = |e_1 g_2 g_3 0\rangle \otimes |\Phi_1\rangle$, and the blue dashed curve is for $|\Psi(0)\rangle = |g_1 e_2 g_3 0\rangle \otimes |\Phi_1\rangle$ or $|\Psi(0)\rangle = |g_1 g_2 e_3 0\rangle \otimes |\Phi_1\rangle$. Firstly, the incident single photon hardly interacts with the first two-level atom when the time t is far earlier than the peak arrival time $t_p = 3$, which is similar to the case when a single photon of Gaussian pulse shape is used to excite a two-level atom; see [36, Fig. 4(a)]. Secondly, the solid red curve is above the solid blue curve for all time. However there is crossover between the dashed curves. Thirdly, the input photon does not affect the steady-state excitation probability of the first TLS (TLS1); however, it does affect the transient dynamics. Finally, from the dashed curves it can be seen that the incident photon tends to increase (or decrease) the excitation probability of the first two-level atom when it is initialized in the ground (or excited) state.

C. Two initially excited atoms plus vacuum input

In the following simulations, we assume that the Tavis-Cummings system is driven by the vacuum input $|\Phi_0\rangle$ and one, two, or even three atoms are initially excited.

We present the following theoretical result first.

Theorem 5.1: Suppose that the Tavis-Cummings system (6) is initialized in the state $|\zeta\rangle = |e_1 \dots e_N 0\rangle$ and driven by the vacuum input field. If $\omega_1 = \dots = \omega_N$ and $\Gamma_1 = \dots = \Gamma_N$, then the steady-state ($t = \infty$) output field must be in an N -photon state.

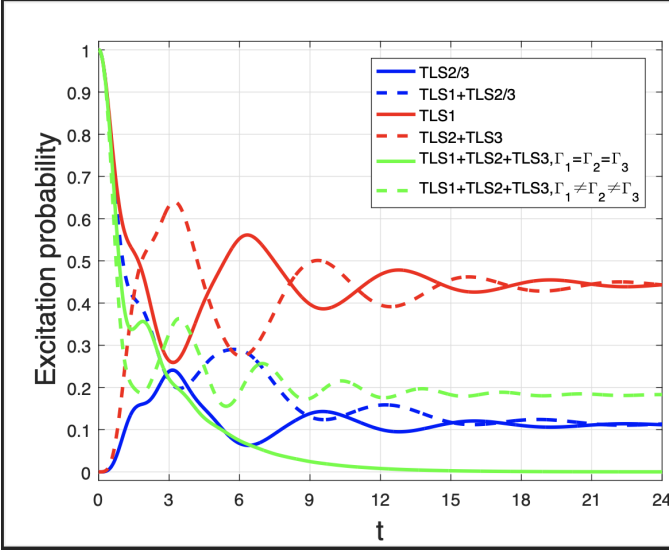


Fig. 4. The excitation probabilities of the first two-level atom. Red solid curve (TLS1: $|e_1 g_2 g_3 0\rangle \otimes |\Phi_0\rangle$); blue solid curve (TLS2/3: $|g_1 e_2 g_3 0\rangle \otimes |\Phi_0\rangle$ or $|g_1 g_2 e_3 0\rangle \otimes |\Phi_0\rangle$); red dashed curve (TLS2 + TLS3: $|g_1 e_2 e_3 0\rangle \otimes |\Phi_0\rangle$); blue dashed curve (TLS1 + TLS2/3: $|e_1 e_2 g_3 0\rangle \otimes |\Phi_0\rangle$ or $|e_1 g_2 e_3 0\rangle \otimes |\Phi_0\rangle$); green solid curve (TLS1+TLS2 + TLS3: $|e_1 e_2 e_3 0\rangle \otimes |\Phi_0\rangle$); green dashed curve (TLS1+TLS2+TLS3: $|e_1 e_2 e_3 0\rangle \otimes |\Phi_0\rangle$ and $\Gamma_1 \neq \Gamma_2 \neq \Gamma_3$).

Proof We use the master equation (51) to prove this result. The steady-state system state can be found by solving

$$\mathcal{L}^* \bar{\rho}^{00}(\infty) = 0. \quad (53)$$

Clearly, in the steady state ($t = \infty$), the cavity cannot contain any photon; otherwise the photon leaks out from the lossy cavity ($\kappa \neq 0$). In other words, such a state cannot be a steady state. Consequently, the steady-state system state is of the form $\bar{\rho}^{00}(\infty) = \rho_A \otimes |0\rangle\langle 0|$, where ρ_A is the steady state of the two-level atoms. By the form of the system Hamiltonian H_{TC} and the coupling operator L given in subsection III-A, (53) is actually

$$\begin{aligned} & \frac{1}{2} \sum_j \omega_j [\sigma_{z,j}, \rho_A] \otimes |0\rangle\langle 0| \\ & + \sum_j \Gamma_j \left(\sigma_{-,j} \rho_A \otimes |1\rangle\langle 0| - \rho_A \sigma_{+,j} |0\rangle\langle 1| \right) = 0. \end{aligned}$$

Given $\omega_1 = \dots = \omega_N \equiv \omega_s$ and $\Gamma_1 = \dots = \Gamma_N \equiv \Gamma$, we have

$$\begin{aligned} & \frac{\omega_s}{2} \sum_j [\sigma_{z,j}, \rho_A] \otimes |0\rangle\langle 0| \\ & + \Gamma \sum_j \left(\sigma_{-,j} \rho_A \otimes |1\rangle\langle 0| - \rho_A \sigma_{+,j} |0\rangle\langle 1| \right) = 0, \end{aligned}$$

which yields

$$\sum_j \sigma_{-,j} \rho_A = 0. \quad (54)$$

In general, ρ_A is of the form

$$\sum_{i_1, \dots, i_N; j_1, \dots, j_N} \alpha_{i_1, \dots, i_N; j_1, \dots, j_N} |f_{i_1} \dots f_{i_N}\rangle \langle g_{j_1} \dots g_{j_N}|,$$

where f_{i_k} and g_{j_k} are either e_k or g_k . Because $\omega_1 = \dots = \omega_N$ and $\Gamma_1 = \dots = \Gamma_N$, all the atoms are indistinguishable. As a result, all the coefficients must be identical; i.e., $\alpha_{i_1, \dots, i_N; j_1, \dots, j_N} \equiv \alpha$ for some α . Consequently,

$$\rho_A = \alpha \sum_{i_1, \dots, i_N; j_1, \dots, j_N} |f_{i_1} \dots f_{i_N}\rangle \langle g_{j_1} \dots g_{j_N}|.$$

Substituting this form of ρ_A into (54) we get $\sigma_{-,j} |f_{i_1} \dots f_{i_N}\rangle = 0$, for all $j = 1, \dots, m$. Clearly, all f_{i_k} must be g_k . Consequently, ρ_A contains a single term and is of the form $\rho_A = |g_1 \dots g_N\rangle \langle g_1 \dots g_N|$. In other words, all atoms are in their ground state. Therefore, in the steady state, the output field is in an N -photon state. \square

The simulation results are shown in Fig. 4. We have the following observations. (i) The first atom's excitation probability when it is initialized in the excited state (the red solid curve) is greater than that when either the second atom or the third atom is initialized in the excited state (the blue solid curve). (ii) The first atom's excitation probability when both the second and third atoms are initialized in the excited state (the red dashed curve) is greater than that when both the first and second atoms (or both the first and third atoms) are initialized in the excited state (the blue dashed curve). (iii) The red solid and dashed curves have the same final value ≈ 0.44 , while the blue solid and dashed curves have the same final value ≈ 0.11 . (iv) The excitation probability of the first two-level atom settles to 0 when all the three atoms are initially excited, see the green solid curve in Fig. 4. Actually, by Theorem 5.1, all the three atoms eventually settle in their ground state and a 3-photon output state is generated. However, if the coupling strengths are not identical, the atoms may not settle to their ground state, as demonstrated by the green dashed curve in Fig. 4, where $\Gamma_1 = 1$, $\Gamma_2 = 1.5$, and $\Gamma_3 = 2$.

Remark 5.2: In Figs. 3 and 4, when the first atom is initialized in the excited state and the other two are in the ground state, the final value of the excitation probability of the first atom is approximately 0.44. By Theorem 4.2, $|c_1(\infty)|^2 = \frac{4}{9}$, which explains this simulation result. The other final value 0.11 in Figs. 3 and 4 can be explained by $|c_2(\infty)|^2 = |c_3(\infty)|^2 = \frac{1}{9}$. Moreover, $|c_k(t)|^2 \rightarrow 1$ and $|c_j(t)|^2 \rightarrow 0$ ($j \neq k$) as $N \rightarrow \infty$. This means that the system tends to remain intact when the number of atoms is sufficiently large. Finally, if $\Gamma_1 = \dots = \Gamma_N$, then by (38) we have $|c_{N+1,k}(\infty)|^2 = \frac{1}{N}$, i.e., only $1/N$ of the excitation energy is radiated. This confirms the analysis in the second paragraph above (29) in [1].

Remark 5.3: Although the red solid and dashed curves have identical stationary excitation probability, their crests and troughs are almost symmetrical during the transient process. Similar phenomena can be observed when $N = 2$. This is consistent with the experimental result given in [4, Fig. 4c]. Specifically, write states $|e_1 g_2\rangle$ and $|g_1 e_2\rangle$ as $|\uparrow\downarrow\rangle$ and $|\downarrow\uparrow\rangle$, respectively. In [4, Fig. 4c], the solid red (green) circles plot the evolution of $|\downarrow\uparrow\rangle$ ($|\uparrow\downarrow\rangle$). The coherent state transfer of the two states emerges and oscillates symmetrically.

VI. A GENERAL FORM OF THE JOINT SYSTEM-FIELD STATES

In Section IV, analytical results are presented for the single-excitation Tavis-Cummings model. These results are not applicable to the multi-excitation case discussed in Section V. Motivated by this, in this section we derive a recursive relation for the computation of the joint system-field state when the system initially contains multiple excitations $R > 1$ and is driven by m input fields initialized in the vacuum state.

A. Modeling

Let H be the internal system Hamiltonian of a quantum system. As the system Hamiltonian may be tuned by a time-varying classical signal, for example, transition frequencies of superconducting qubits can be tuned via Josephson energy in Josephson-junction-based superconducting circuits [37], we use $H(t)$ to emphasize the explicit dependence of the system Hamiltonian on time. The coupling between the quantum system and the k th ($k = 1, \dots, m$) input channel can be described by a coupling operator $L_k(t)$; again, here we allow explicit time dependence of the coupling as in some quantum systems couplings can be tuned in real time [38].

The system of interest may be an ensemble of TLSs, or resonators, or even an ensemble of TLSs residing in a resonator like the Tavis-Cummings model studied in this paper. If the number of TLSs is finite, the number of photons in the resonator is finite, and the system is driven by a finite number of photons, then the number of total excitations R in the whole system (the system plus the external field) is finite too. In this case, the state of the quantum system has an orthonormal basis of the form

$$\{|0_s\rangle, \dots, |(K-1)_s\rangle\}, \quad (55)$$

where the subscript “ s ” indicates that the basis states $|j_s\rangle$, $j = 0, 1, \dots, K-1$, are for the system. For our Tavis-Cummings mode in Fig. 1, $K = 2^N(R+1)$ as each of the N atoms has two basis states and the cavity can contain at most R photons.

Remark 6.1: If the system of interest is coherently driven, then the number of excitations can be arbitrary large as the drive may generate an arbitrary number of excitations. However, if the coherent drive is not very strong and lasts not long, the number of excitations in the system will be upper bounded. Hence, it can still be assumed that the system admits a basis of finitely many elements.

For notational convenience, the following notation will be adopted. For each $i = 1, \dots, m$, we use $t_{1 \rightarrow k_i}^i$ to denote a set of ordered real numbers $\{t_1^i, \dots, t_{k_i}^i : t_1^i < \dots < t_{k_i}^i\}$. Similarly, $1_{t_{1 \rightarrow k_j}^j}$ is a shorthand of $1_{t_1^j}, \dots, 1_{t_{k_j}^j}$. Let $\int_r^{t^i \rightarrow k_i}$ be the abbreviation for $\int_r^{t_{k_i}^i} \dots \int_r^{t_1^i}$. Finally, for each given non-negative integer n , \sum_{k_1, \dots, k_m}^n means the summation over all possible combinations of the non-negative integers k_1, \dots, k_m that satisfy $\sum_{j=1}^m k_j = n$.

The temporal photon-number basis of n photons superposed over m channels is

$$\left\{ |1_{t_1^1}\rangle \otimes \dots \otimes |1_{t_{k_1}^1}\rangle \otimes \dots \otimes |1_{t_1^m}\rangle \otimes \dots \otimes |1_{t_{k_m}^m}\rangle : \right. \\ \left. t_1^1 < \dots < t_{k_1}^1, \dots, t_1^m < \dots < t_{k_m}^m, \sum_{i=1}^m k_i = n \right\}, \quad (56)$$

where k_1, \dots, k_m are non-negative integers. Particularly, if $k_i = 0$, then there are no photons in channel i and correspondingly the term $|1_{t_1^1}\rangle \otimes \dots \otimes |1_{t_{k_i}^i}\rangle$ reduces to $|\Phi_0\rangle$. As a common practice in quantum physics, the tensor product state in (56) is often written as $|1_{t_1^1}, \dots, 1_{t_{k_1}^1}, \dots, 1_{t_1^m}, \dots, 1_{t_{k_m}^m}\rangle$, which is $|1_{t_{1 \rightarrow k_1}^1}, \dots, 1_{t_{1 \rightarrow k_m}^m}\rangle$ by means of the notation given in the last paragraph.

Using the temporal photon-number basis in (56), an m -channel n -photon state can be written as

$$|n_\xi\rangle = \sum_{k_1, \dots, k_m}^n \int_{-\infty}^{\infty} \dots \int_{-\infty}^{\infty} \xi(t_{1 \rightarrow k_1}^1, \dots, t_{1 \rightarrow k_m}^m) \\ |1_{t_{1 \rightarrow k_1}^1}, \dots, 1_{t_{1 \rightarrow k_m}^m}\rangle dt_{1 \rightarrow k_1}^1 \dots dt_{1 \rightarrow k_m}^m, \quad (57)$$

where the j th channel has k_j photons, and $\sum_{j=1}^m k_j = n$ is the total photon number. Clearly, $\xi(t_{1 \rightarrow k_1}^1, \dots, t_{1 \rightarrow k_m}^m)$ is the probability amplitude of the component that the j th channel has photons at time instants $t_1^j, \dots, t_{k_j}^j$ for all $j = 1, \dots, m$.

Due to the indistinguishability of photons in each channel, for each fixed $j = 1, \dots, m$, $\xi(t_{1 \rightarrow k_1}^1, \dots, t_{1 \rightarrow k_m}^m)$ is permutation-invariant with respect to indices $\{t_{1 \rightarrow k_j}^j\}$. Thus, under scaling $\frac{1}{k_1! \dots k_m!}$, the state $|n_\xi\rangle$ can be rewritten as

$$|n_\xi\rangle = \sum_{k_1, \dots, k_m}^n \int_{-\infty}^{\infty} \int_{-\infty}^{t_{2 \rightarrow k_1}^1} \dots \int_{-\infty}^{\infty} \int_{-\infty}^{t_{2 \rightarrow k_m}^m} \xi(t_{1 \rightarrow k_1}^1, \dots, t_{1 \rightarrow k_m}^m) \\ |1_{t_{1 \rightarrow k_1}^1}, \dots, 1_{t_{1 \rightarrow k_m}^m}\rangle dt_{1 \rightarrow k_1}^1 \dots dt_{1 \rightarrow k_m}^m. \quad (58)$$

In fact, one can always define an n -photon state using (58) with an arbitrary multivariate function $\xi(t_{1 \rightarrow k_1}^1, \dots, t_{1 \rightarrow k_m}^m)$ (under normalization), then obtain the form in (57) by permutating indices $\{t_{1 \rightarrow k_j}^j\}$ for all $j = 1, \dots, m$. The form of n -photon states (58) is more often to see in practice than that in (57). For example, by applying a coherent drive to a superconducting qubit embedded in a chiral waveguide, the qubit may generate photon states of the form (58). Therefore, in what follows we use (58) to describe n -photon states.

B. The general form

In this subsection, we present a computational procedure that can be used to compute the joint system-field state. Some other computational framework can be found in e.g., [40], [41].

The basis state of the joint system-field state when the system is at level $|j_s\rangle$ and channel i has k_i photons at time

instants $t_{1 \rightarrow k_i}^i$ is $|j_s\rangle \otimes |1_{t_{1 \rightarrow k_1}}^1, \dots, 1_{t_{1 \rightarrow k_m}}^m\rangle$. Hence, the joint system-field state is of the general form

$$|\Psi\rangle = \sum_{j=0}^{K-1} \sum_{n=0}^{\infty} \sum_{k_1, \dots, k_m}^n \int_{-\infty}^{\infty} \int_{-\infty}^{t_{2 \rightarrow k_1}^1} \dots \int_{-\infty}^{\infty} \int_{-\infty}^{t_{2 \rightarrow k_m}^m} \xi^{j_s}(t_{1 \rightarrow k_1}^1, \dots, t_{1 \rightarrow k_m}^m) |j_s\rangle dB_{\text{in},1}^*(t_{1 \rightarrow k_1}^1) \dots dB_{\text{in},m}^*(t_{1 \rightarrow k_m}^m) |\Phi_0\rangle, \quad (59)$$

where we write informally $dB_{\text{in},k}^*(t) = b_{\text{in},k}^*(t)dt$ and $dB_{\text{in},i}^*(t_{1 \rightarrow k_i}^i)$ as the product $dB_{\text{in},i}^*(t_1^i) \dots dB_{\text{in},i}^*(t_{k_i}^i)$. The normalization condition $\langle \Psi | \Psi \rangle = 1$ gives

$$\sum_{j=0}^{K-1} \sum_{n=0}^{\infty} \sum_{k_1, \dots, k_m}^n \int_{-\infty}^{\infty} \int_{-\infty}^{t_{2 \rightarrow k_1}^1} \dots \int_{-\infty}^{\infty} \int_{-\infty}^{t_{2 \rightarrow k_m}^m} |\xi^{j_s}(t_{1 \rightarrow k_1}^1, \dots, t_{1 \rightarrow k_m}^m)|^2 dt_{1 \rightarrow k_1}^1 \dots dt_{1 \rightarrow k_m}^m = 1.$$

Denote

$$|\eta(t_{1 \rightarrow k_1}^1, \dots, t_{1 \rightarrow k_m}^m)\rangle = \sum_{j=0}^{K-1} \xi^{j_s}(t_{1 \rightarrow k_1}^1, \dots, t_{1 \rightarrow k_m}^m) |j_s\rangle.$$

It is worthwhile to note that $|\eta(t_{1 \rightarrow k_1}^1, \dots, t_{1 \rightarrow k_m}^m)\rangle$ in general is not normalized. The state $|\Psi\rangle$ in (59) can be re-written as

$$|\Psi\rangle = \sum_{n=0}^{\infty} \sum_{k_1, \dots, k_m}^n \int_{-\infty}^{\infty} \int_{-\infty}^{t_{2 \rightarrow k_1}^1} \dots \int_{-\infty}^{\infty} \int_{-\infty}^{t_{2 \rightarrow k_m}^m} |\eta(t_{1 \rightarrow k_1}^1, \dots, t_{1 \rightarrow k_m}^m)\rangle dB_{\text{in},1}^*(t_{1 \rightarrow k_1}^1) \dots dB_{\text{in},m}^*(t_{1 \rightarrow k_m}^m) |\Phi_0\rangle.$$

If the input field is initially in the vacuum state $|\Phi_0\rangle$, then the initial joint system-field state is $|\Psi(t_0)\rangle = \sum_{j=0}^{K-1} \xi^{j_s} |j_s\rangle \otimes |\Phi_0\rangle \equiv |\eta_0\rangle \otimes |\Phi_0\rangle$, where $\sum_{j=0}^{K-1} |\xi^{j_s}|^2 = 1$. Because the photon generation time is from the initial time $t_0 = 0$ to the present time $t > 0$, the joint system-field state at time t is

$$|\Psi(t)\rangle = \sum_{n=0}^{\infty} \sum_{k_1, \dots, k_m}^n \int_0^t \int_0^{t_{2 \rightarrow k_1}^1} \dots \int_0^t \int_0^{t_{2 \rightarrow k_m}^m} |\eta_t(t_{1 \rightarrow k_1}^1, \dots, t_{1 \rightarrow k_m}^m)\rangle dB_{\text{in},1}^*(t_{1 \rightarrow k_1}^1) \dots dB_{\text{in},m}^*(t_{1 \rightarrow k_m}^m) |\Phi_0\rangle, \quad (60)$$

where

$$|\eta_t(t_{1 \rightarrow k_1}^1, \dots, t_{1 \rightarrow k_m}^m)\rangle = \sum_{j=0}^{K-1} \xi_t^{j_s}(t_{1 \rightarrow k_1}^1, \dots, t_{1 \rightarrow k_m}^m) |j_s\rangle. \quad (61)$$

(Here, the subscript “ t ” indicates that the coefficients are time dependent.) In particular, the term in $|\Psi(t)\rangle$ that corresponds to $n = 0$ is $|\eta_t\rangle |\Phi_0\rangle = \sum_{j=0}^{K-1} \xi_t^{j_s} |j_s\rangle |\Phi_0\rangle$. In other words, the field is in the vacuum state and the system is in the superposition state $\sum_{j=0}^{K-1} \xi_t^{j_s} |j_s\rangle$.

In what follows, we aim to derive formulas for computing the joint system-field state $|\Psi(t)\rangle$. Differentiating both sides of (60) yields

$$\begin{aligned} d|\Psi(t)\rangle &= \sum_{n=1}^{\infty} \sum_{k_1, \dots, k_m}^n dB_{\text{in},1}^*(t) \int_0^t \int_0^{t_{2 \rightarrow k_1}^1} \dots \int_0^t \int_0^{t_{2 \rightarrow k_m}^m} |\eta_t(t_{1 \rightarrow k_1}^1, \dots, t_{2 \rightarrow k_2}^2, \dots, t_{1 \rightarrow k_m}^m)\rangle dB_{\text{in},1}^*(t_{1 \rightarrow k_1}^1) \dots dB_{\text{in},m}^*(t_{1 \rightarrow k_m}^m) |\Phi_0\rangle \\ &\vdots \\ &+ \sum_{n=1}^{\infty} \sum_{k_1, \dots, k_m}^n dB_{\text{in},m}^*(t) \int_0^t \int_0^{t_{2 \rightarrow k_1}^1} \dots \int_0^t \int_0^{t_{2 \rightarrow k_{m-1}}^m} |\eta_t(t_{1 \rightarrow k_1}^1, \dots, t_{1 \rightarrow k_{m-1}}^{m-1}, t_{1 \rightarrow k_m}^m, t)\rangle dB_{\text{in},1}^*(t_{1 \rightarrow k_1}^1) \dots dB_{\text{in},m}^*(t_{1 \rightarrow k_{m-1}}^m) |\Phi_0\rangle \\ &+ dt \sum_{n=0}^{\infty} \sum_{k_1, \dots, k_m}^n \int_{-\infty}^{\infty} \int_{-\infty}^{t_{2 \rightarrow k_1}^1} \dots \int_{-\infty}^{\infty} \int_{-\infty}^{t_{2 \rightarrow k_m}^m} |\dot{\eta}_t(t_{1 \rightarrow k_1}^1, \dots, t_{1 \rightarrow k_m}^m)\rangle dB_{\text{in},1}^*(t_{1 \rightarrow k_1}^1) \dots dB_{\text{in},m}^*(t_{1 \rightarrow k_m}^m) |\Phi_0\rangle, \end{aligned} \quad (62)$$

where $\dot{\eta}_t$ means the derivative of η with respect to t . Comparing the right-hand sides of (62) and (3) (for $|\Psi(t)\rangle$ in (60)), we get

$$|\dot{\eta}_t(t_{1 \rightarrow k_1}^1, \dots, t_{1 \rightarrow k_m}^m)\rangle = -iH_{\text{eff}}(t) |\eta_t(t_{1 \rightarrow k_1}^1, \dots, t_{1 \rightarrow k_m}^m)\rangle, \quad (63)$$

and

$$|\eta_t(t_{1 \rightarrow k_1}^1, \dots, t_{1 \rightarrow k_i}^i, t, \dots, t_{1 \rightarrow k_m}^m)\rangle = L_i(t) |\eta_t(t_{1 \rightarrow k_1}^1, \dots, t_{1 \rightarrow k_i}^i, \dots, t_{1 \rightarrow k_m}^m)\rangle \quad (64)$$

for all $i = 1, \dots, m$. Under the basis (55), the effective Hamiltonian H_{eff} of the system has a matrix representation. Hence, similar to what has been done in [13], define the propagator $V(t)$ (a matrix function) that solves a system of deterministic homogeneous ODEs $\dot{V}(t) = -iH_{\text{eff}}(t)V(t)$ under the initial condition $V(0) = I$. Then one can define the transition matrix

$$G(t, \tau) \triangleq V(t)V(\tau)^{-1}, \quad t, \tau \geq 0. \quad (65)$$

Clearly, for the 0 photon state case, (63) and (65) yield

$$|\eta_t\rangle = G(t, 0) |\eta_0\rangle, \quad t \geq 0. \quad (66)$$

As is well-known in linear systems theory, see e.g. [42, Chapter 4], iteratively using the transition matrix $G(t, \tau)$ in

(65) and (64) we have

$$\begin{aligned}
& |\eta_t(t_1^{1 \rightarrow k_1}, t_1^{2 \rightarrow k_2}, \dots, t_1^{m \rightarrow k_m})\rangle \\
&= G(t, t_{k_1}^1) |\eta_{t_{k_1}^1}(t_1^{1 \rightarrow k_1-1}, t_{k_1}^1, t_1^{2 \rightarrow k_2}, \dots, t_1^{m \rightarrow k_m})\rangle \\
&= G(t, t_{k_1}^1) L_1(t_{k_1}^1) |\eta_{t_{k_1}^1}(t_1^{1 \rightarrow k_1-1}, t_1^{2 \rightarrow k_2}, \dots, t_1^{m \rightarrow k_m})\rangle \\
&= G(t, t_{k_1}^1) L_1(t_{k_1}^1) G(t_{k_1}^1, t_{k_1-1}^1) \\
&\quad \times |\eta_{t_{k_1-1}^1}(t_1^{1 \rightarrow k_1-1}, t_1^{2 \rightarrow k_2}, \dots, t_1^{m \rightarrow k_m})\rangle \\
&\vdots \\
&= G(t, t_{k_1}^1) L_1(t_{k_1}^1) \cdots G(t_2^1, t_1^1) L_1(t_1^1) \\
&\quad \times G(t_1^1, t_{k_2}^2) |\eta_{t_{k_2}^2}(t_1^{2 \rightarrow k_2}, \dots, t_1^{m \rightarrow k_m})\rangle \\
&\vdots \\
&= G(t, t_{k_1}^1) L_1(t_{k_1}^1) \cdots G(t_2^1, t_1^1) L_1(t_1^1) G(t_1^1, t_{k_2}^2) L_2(t_{k_2}^2) \times \cdots \\
&\quad \times G(t_2^2, t_1^2) L_2(t_1^2) G(t_1^2, t_{k_3}^3) |\eta_{t_{k_3}^3}(t_1^{3 \rightarrow k_3}, \dots, t_1^{m \rightarrow k_m})\rangle \\
&\vdots \\
&= G(t, t_{k_1}^1) L_1(t_{k_1}^1) \cdots G(t_2^1, t_1^1) L_1(t_1^1) \\
&\quad \times G(t_1^1, t_{k_2}^2) L_2(t_{k_2}^2) \cdots G(t_2^2, t_1^2) L_2(t_1^2) \times \cdots \\
&\quad \times G(t_1^{m-1}, t_{k_m}^m) L_m(t_{k_m}^m) \cdots G(t_2^m, t_1^m) L_m(t_1^m) G(t_1^m, 0) |\eta_0\rangle.
\end{aligned}$$

Consequently, we have the following general formula

$$\begin{aligned}
& |\eta_t(t_1^{1 \rightarrow k_1}, t_1^{2 \rightarrow k_2}, \dots, t_1^{m \rightarrow k_m})\rangle \\
&= G(t, t_{k_1}^1) L_1(t_{k_1}^1) \cdots G(t_2^1, t_1^1) L_1(t_1^1) \\
&\quad \times G(t_1^1, t_{k_2}^2) L_2(t_{k_2}^2) \cdots G(t_2^2, t_1^2) L_2(t_1^2) \cdots \\
&\quad \times G(t_1^{m-1}, t_{k_m}^m) L_m(t_{k_m}^m) \cdots G(t_2^m, t_1^m) L_m(t_1^m) \\
&\quad \times G(t_1^m, 0) |\eta_0\rangle.
\end{aligned} \tag{67}$$

Remark 6.2: To better understand the recursive algorithm given in (67), we take the two-channel case as an example, i.e., $m = 2$. In this case, the first channel contains k_1 photons and the second channel contains k_2 photons. The recursive functions (63) and (64) are reduced to be

$$|\dot{\eta}_t^{k_1, k_2}(t_1^{1 \rightarrow k_1}, t_1^{2 \rightarrow k_2})\rangle = -iH_{\text{eff}}(t) |\eta_t^{k_1, k_2}(t_1^{1 \rightarrow k_1}, t_1^{2 \rightarrow k_2})\rangle, \tag{68}$$

and

$$\begin{aligned}
& |\eta_t^{k_1+1, k_2}(t_1^{1 \rightarrow k_1}, t, t_1^{2 \rightarrow k_2})\rangle = L_1(t) |\eta_t^{k_1, k_2}(t_1^{1 \rightarrow k_1}, t_1^{2 \rightarrow k_2})\rangle, \\
& |\eta_t^{k_1, k_2+1}(t_1^{1 \rightarrow k_1}, t_1^{2 \rightarrow k_2}, t)\rangle = L_2(t) |\eta_t^{k_1, k_2}(t_1^{1 \rightarrow k_1}, t_1^{2 \rightarrow k_2})\rangle.
\end{aligned} \tag{69}$$

According to (67), we have

$$\begin{aligned}
& |\eta_t^{k_1, k_2}(t_1^{1 \rightarrow k_1}, t_1^{2 \rightarrow k_2})\rangle \\
&= G(t, t_{k_1}^1) L_1(t_{k_1}^1) \cdots G(t_2^1, t_1^1) L_1(t_1^1) \\
&\quad \times G(t_1^1, t_{k_2}^2) L_2(t_{k_2}^2) \cdots G(t_2^2, t_1^2) L_2(t_1^2) \\
&\quad \times G(t_1^2, 0) |\eta_0\rangle,
\end{aligned} \tag{70}$$

which yields

$$\begin{aligned}
& |\eta_t\rangle = G(t, 0) |\eta_0\rangle, \\
& |\eta_t^{1,0}(t_1^1)\rangle = G(t, t_1^1) L_1(t_1^1) G(t_1^1, 0) |\eta_0\rangle, \\
& |\eta_t^{0,1}(t_2^1)\rangle = G(t, t_1^1) L_2(t_1^1) G(t_1^1, 0) |\eta_0\rangle, \\
& |\eta_t^{1,1}(t_1^1, t_2^1)\rangle = G(t, t_1^1) L_1(t_1^1) G(t_1^1, t_2^1) L_2(t_2^1) G(t_2^1, 0) |\eta_0\rangle \\
&\quad = G(t, t_1^1) L_2(t_1^1) G(t_1^1, t_2^1) L_1(t_2^1) G(t_2^1, 0) |\eta_0\rangle, \\
&\quad \vdots
\end{aligned} \tag{71}$$

That is, there are multiple sequential orders to generate a $(k_1 + k_2)$ -photon state distributed in two channels ($k_1, k_2 \geq 1$), which allow the two channels being created crosswise.

The following recursive relation turns out useful for deriving all the states.

$$\begin{aligned}
& |\eta_t(t_1^{1 \rightarrow k_1}, \dots, t_1^{i \rightarrow k_i+1}, \dots, t_1^{m \rightarrow k_m})\rangle \\
&= G(t, t_{k_i+1}^i) L_i(t_{k_i+1}^i) G(t, t_{k_i+1}^i)^{-1} \\
&\quad |\eta_t(t_1^{1 \rightarrow k_1}, \dots, t_1^{i \rightarrow k_i}, \dots, t_1^{m \rightarrow k_m})\rangle.
\end{aligned} \tag{72}$$

Remark 6.3: Theorem 4.2 in Section IV-C can be proved by applying the recursive relation (72) to the special case when $m = 1$ and the initial system-field state is

$$|\Psi(0)\rangle = |\Psi_k(0)\rangle = |\eta_0\rangle \otimes |\Phi_0\rangle, \tag{73}$$

where $|\eta_0\rangle = |g_1 \cdots e_k \cdots g_N 0\rangle$. In what follows we sketch the proof. Because there is only one input channel and the number of excitation is 1, i.e., $m = 1$ and $k_1 = 1$, the joint system-field state $|\Psi(t)\rangle$ in (60) is

$$|\Psi(t)\rangle = |\eta_t\rangle \otimes |\Phi_0\rangle + \int_0^t |\eta_t(t_1)\rangle dB_{\text{in}}^*(t_1) \otimes |\Phi_0\rangle. \tag{74}$$

The first term in (74) indicates that the single excitation exists in the Tavis-Cummings model. $|\eta_t\rangle$ can be described by

$$|\eta_t\rangle = \sum_{j=1}^N c_j(t) |g_1 \cdots e_j \cdots g_N 0\rangle + c_{N+2,k}(t) |g_1 g_2 \cdots g_N 1\rangle$$

with the initial conditions $c_k(0) = 1$ and $c_j(0) = c_{N+2,k}(0) = 0$ for $1 \leq j \leq N$, $j \neq k$. On the other hand, the second term in (74) means that the Tavis-Cummings model emits a photon into the output field, which can be rewritten as

$$\begin{aligned}
& \int_0^t |\eta_t(t_1)\rangle dB_{\text{in}}^*(t_1) \otimes |\Phi_0\rangle \\
&= c_{N+1}(t) \int_0^t \varphi(t_1) dB_{\text{in}}^*(t_1) |g_1 g_2 \cdots g_N 0\rangle \otimes |\Phi_0\rangle.
\end{aligned}$$

Here, $\varphi(t_1)$ is the pulse shape of the single-photon output state. When $t \rightarrow \infty$, $c_{N+1}(\infty)$ denotes the probability amplitude corresponding to the reduced joint state $|g_1 g_2 \cdots g_N 0\rangle \otimes |\Phi_1\rangle$. By the recursive relation (72), we have $|\eta_t(t_1)\rangle = G(t, t_1) L_1(t_1) G(t, t_1)^{-1} |\eta_t\rangle$, where $|\eta_t\rangle$ can be calculated via (66) and (73). Theorem 4.2 follows.

In the following subsections, we apply the above theory to our Tavis-Cummings model. In this case, $m = 1$, $L_i(t)$ in (64) is $L = \sqrt{\kappa}a$, and $H_{\text{eff}}(t)$ in (63) is $H_{\text{TC}} - \frac{i}{2}L^*L$, where H_{TC} is given in (5). For simplicity, we set $\omega_1 = \dots = \omega_N \equiv \omega_r = 0$ and $\Gamma_1 = \dots = \Gamma_N = \kappa = 1$. Assume that the

Tavis-Cummings model contains R initially excited two-level atoms, the cavity is initially empty, and the input is in the vacuum state. In such setting, the number of basis states of the Tavis-Cummings model is $K = 2^N(R + 1)$ as discussed in subsection VI-A. Finally, for better illustration we plot the symmetric pulse shape in (57), instead of that in (58).

C. $N = 3$ and $R = 1$.

In this case, the total number of basis states is $K = 16$. The joint system-field state can be expressed as $|\Psi(t)\rangle = |\eta_t\rangle \otimes |\Phi_0\rangle + \int_0^t |\eta_t(t_1)\rangle dB_{\text{in}}^*(t_1) |\Phi_0\rangle$, where by (61), $|\eta_t(t_1, \dots, t_k)\rangle = \sum_{j=0}^{15} \xi_t^{j_s}(t_1, \dots, t_k) |j_s\rangle$, $k = 0, 1$. Let the initial joint system-field state be $|\Psi(0)\rangle = |e_1 g_2 g_3 0\rangle \otimes |\Phi_0\rangle$. By the recursive relation (72), we have

$$\begin{aligned}\xi_t^{1_s} &= \frac{2}{\sqrt{47}} \left(e^{\frac{-1-\sqrt{47}i}{4}t} - e^{\frac{-1+\sqrt{47}i}{4}t} \right), \\ \xi_t^{2_s} &= -\frac{1}{3} + \frac{2 \left(\frac{\sqrt{47}+i}{4} e^{\frac{-1-\sqrt{47}i}{4}t} + \frac{\sqrt{47}-i}{4} e^{\frac{-1+\sqrt{47}i}{4}t} \right)}{3\sqrt{47}}, \\ \xi_t^{4_s} &= \xi_t^{2_s}, \\ \xi_t^{8_s} &= \frac{2}{3} + \frac{2 \left(\frac{\sqrt{47}+i}{4} e^{\frac{-1-\sqrt{47}i}{4}t} + \frac{\sqrt{47}-i}{4} e^{\frac{-1+\sqrt{47}i}{4}t} \right)}{3\sqrt{47}}, \\ \xi_t^{0_s}(t_1) &= -\frac{4i}{\sqrt{47}} e^{-\frac{1}{4}t_1} \sin\left(\frac{\sqrt{47}}{4}t_1\right), \quad 0 \leq t_1 \leq t,\end{aligned}$$

and all the others are 0. In the steady state ($t = \infty$), we have $\xi_\infty^{2_s} = \xi_\infty^{4_s} = -\frac{1}{3}$, $\xi_\infty^{8_s} = \frac{2}{3}$, which correspond to the basis vectors $|g_1 g_2 e_3 0\rangle$, $|g_1 e_2 g_3 0\rangle$, $|e_1 g_2 g_3 0\rangle$ respectively. Moreover, as $\lim_{t \rightarrow \infty} \int_0^\infty |\xi_t^{0_s}(t_1)|^2 dt_1 = \frac{1}{3}$, the steady-state joint system-field state is

$$\begin{aligned}|\Psi(\infty)\rangle &= \frac{2}{3} |e_1 g_2 g_3 0\rangle \otimes |\Phi_0\rangle - \frac{1}{3} |g_1 e_2 g_3 0\rangle \otimes |\Phi_0\rangle \\ &\quad - \frac{1}{3} |g_1 g_2 e_3 0\rangle \otimes |\Phi_0\rangle + \frac{1}{\sqrt{3}} |g_1 g_2 g_3 0\rangle \otimes |1_\eta\rangle,\end{aligned}\quad (75)$$

where the pulse shape of the single photon is $\eta(t) = \sqrt{3}\xi_\infty^{0_s}(t)$ up to a global phase. Finally, the square of the probability amplitude $2/3$ in (75) is consistent with the limiting value of the red solid curve in Fig. 4.

D. $N = 2$ and $R = 2$.

In this case, the total number of basis states is $K = 12$. The joint system-field state can be expressed as

$$\begin{aligned}|\Psi(t)\rangle &= |\eta_t\rangle \otimes |\Phi_0\rangle + \int_0^t |\eta_t(t_1)\rangle dB_{\text{in}}^*(t_1) |\Phi_0\rangle \\ &\quad + \int_0^t \int_0^{t_2} |\eta_t(t_1, t_2)\rangle dB_{\text{in}}^*(t_1) dB_{\text{in}}^*(t_2) |\Phi_0\rangle,\end{aligned}$$

where $|\eta_t(t_1, \dots, t_k)\rangle = \sum_{j=0}^{11} \xi_t^{j_s}(t_1, \dots, t_k) |j_s\rangle$, $k = 0, 1, 2$. Let the initial joint system-field state be $|\Psi(0)\rangle = |e_1 e_2 0\rangle \otimes |\Phi_0\rangle$. By Theorem 5.1, the steady-state joint system-field state ($t \rightarrow \infty$) is

$$|\Psi(\infty)\rangle = |g_1 g_2 0\rangle \otimes |2_\eta\rangle, \quad (76)$$

where $|2_\eta\rangle$ is the 2-photon output state. By the recursive relation (72), the pulse shape of the 2-photon state $|2_\eta\rangle$ is

$$\begin{aligned}\eta(t_1, t_2) &= \xi_\infty^{0_s}(t_1, t_2) \\ &= (0.0228787 - 0.00785441i) e^{\mu_1 t_1 - \mu_4 t_2} \\ &\quad + (0.319599 + 0.0291387i) e^{\mu_2 t_1 - \mu_4 t_2} \\ &\quad - (0.342477 + 0.0212843i) e^{\mu_3 t_1 - \mu_4 t_2} + \text{c.c.},\end{aligned}$$

where “c.c.” means complex conjugate, and $\mu_1 = -0.336506 + 3.79453i$, $\mu_2 = -0.336506 - 1.01065i$, $\mu_3 = -0.076987 + 1.39194i$, and $\mu_4 = 0.25 + 1.39194i$. It can be easily verified that $\int_0^\infty \int_0^{t_2} |\eta(t_1, t_2)|^2 dt_1 dt_2 = 1$. The probability distribution of the steady-state output two-photon state $|2_\eta\rangle$ in (76) is simulated in Fig. 5.

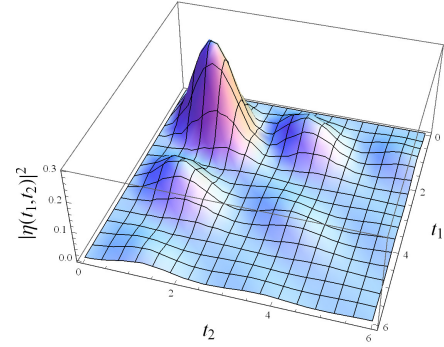


Fig. 5. Probability distribution of $|2_\eta\rangle$ in (76).

E. $N = 3$ and $R = 2$.

In this case, the total number of basis states is $K = 24$. The joint system-field state can be expressed as

$$\begin{aligned}|\Psi(t)\rangle &= |\eta_t\rangle \otimes |\Phi_0\rangle + \int_0^t |\eta_t(t_1)\rangle dB_{\text{in}}^*(t_1) |\Phi_0\rangle \\ &\quad + \int_0^t \int_0^{t_2} |\eta_t(t_1, t_2)\rangle dB_{\text{in}}^*(t_1) dB_{\text{in}}^*(t_2) |\Phi_0\rangle,\end{aligned}$$

where $|\eta_t(t_1, \dots, t_k)\rangle = \sum_{j=0}^{23} \xi_t^{j_s}(t_1, \dots, t_k) |j_s\rangle$, $k = 0, 1, 2$. Let the initial joint system-field state be $|\Psi(0)\rangle = |g_1 e_2 e_3 0\rangle \otimes |\Phi_0\rangle$. According to the recursive relation (72), we have the steady-state joint system-field state

$$\begin{aligned}|\Psi(\infty)\rangle &= \frac{2}{3} |e_1 g_2 g_3 0\rangle \otimes |1_{\eta^{12_s}}\rangle + \frac{1}{3} |g_1 e_2 g_3 0\rangle \otimes |1_{\eta^{6_s}}\rangle \\ &\quad + \frac{1}{3} |g_1 g_2 e_3 0\rangle \otimes |1_{\eta^{3_s}}\rangle + \frac{\sqrt{3}}{3} |g_1 g_2 g_3 0\rangle \otimes |2_{\eta^{0_s}}\rangle,\end{aligned}\quad (77)$$

where $\eta^{12_s}(t) = \frac{3}{2}\xi_\infty^{12_s}(t) = 0.5163975 (e^{\lambda' t} - e^{\lambda'^* t})$ with $\lambda' = -0.25 + 0.968246i$, $\eta^{6_s}(t) = \eta^{3_s}(t) = -\eta^{12_s}(t)$, and $\eta^{0_s}(t_1, t_2) = \sqrt{3}\xi_\infty^{0_s}(t_1, t_2)$

$$\begin{aligned}&= (0.338571 + 0.0140041i) e^{\lambda'_1 t_1 - \lambda'_4 t_2} \\ &\quad + (0.0155773 - 0.00341903i) e^{\lambda'_2 t_1 - \lambda'_4 t_2} \\ &\quad - (0.354149 + 0.0105851i) e^{\lambda'_3 t_1 - \lambda'_4 t_2} + \text{c.c.}\end{aligned}$$

with $\lambda'_1 = -0.301227 - 1.40985i$, $\lambda'_2 = -0.301227 + 4.83767i$, $\lambda'_3 = -0.147546 + 1.71391i$, and $\lambda'_4 = 0.25 +$

1.71391i. The square of the probability amplitude $\frac{2}{3}$ in (77) is consistent with the limiting value of the red dashed curve in Fig. 4. It is clear in Fig. 6 that $|1_\eta\rangle$ has more oscillations than $|1_{\eta^{12s}}\rangle$.

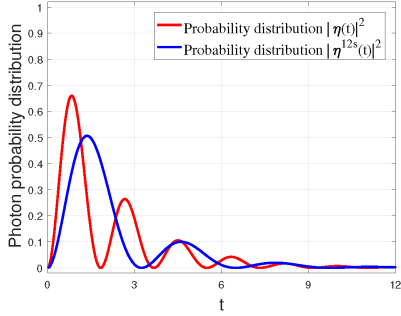


Fig. 6. The comparison between probability distributions of the steady-state single-photon output states $|1_\eta\rangle$ in (75) and $|1_{\eta^{12s}}\rangle$ in (77).

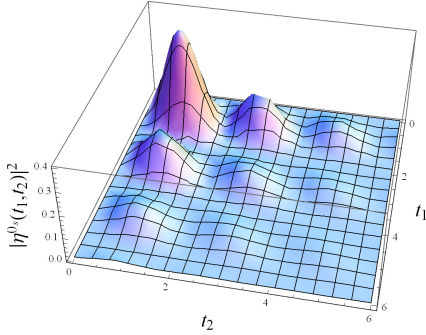


Fig. 7. Probability distribution of the two-photon output state $|2_{\eta^0s}\rangle$ in (77).

Both Figs. 5 and 7 show the probability distributions of a two-photon output state. The one generated by the Tavis-Cummings system with 3 atoms (shown in Fig. 7) oscillates more rapidly than that with 2 atoms (see Fig. 5). This result indicates that the Rabi oscillation is enhanced by adding more atoms, which is consistent with the discussions in Fig. 2 and the observations in [43, Fig. 5].

F. $N = 3$ and $R = 3$.

In this case, the total number of basis states is $K = 32$ and the joint system-field state can be expressed as

$$\begin{aligned} |\Psi(t)\rangle &= |\eta_t\rangle \otimes |\Phi_0\rangle + \int_0^t |\eta_t(t_1)\rangle dB_{\text{in}}^*(t_1) |\Phi_0\rangle \\ &+ \int_0^t \int_0^{t_2} |\eta_t(t_1, t_2)\rangle dB_{\text{in}}^*(t_1) dB_{\text{in}}^*(t_2) |\Phi_0\rangle \\ &+ \int_0^t \int_0^{t_2} \int_0^{t_3} |\eta_t(t_1, t_2, t_3)\rangle dB_{\text{in}}^*(t_1) dB_{\text{in}}^*(t_2) dB_{\text{in}}^*(t_3) |\Phi_0\rangle, \end{aligned}$$

where $|\eta_t(t_1, \dots, t_k)\rangle = \sum_{j=0}^{31} \xi_t^{j_s}(t_1, \dots, t_k) |j_s\rangle$, $k = 0, 1, 2, 3$. Since the three atoms are all initially excited, the initial joint system-field state is $|\Psi(0)\rangle = |e_1 e_2 e_3 0\rangle \otimes |\Phi_0\rangle$. By Theorem 5.1, the steady-state joint system-field state is

$$|\Psi(\infty)\rangle = |g_1 g_2 g_3 0\rangle \otimes |3_\eta\rangle, \quad (78)$$

where $|3_\eta\rangle$ is the three-photon output state, whose probability distribution is shown in Fig. 8.

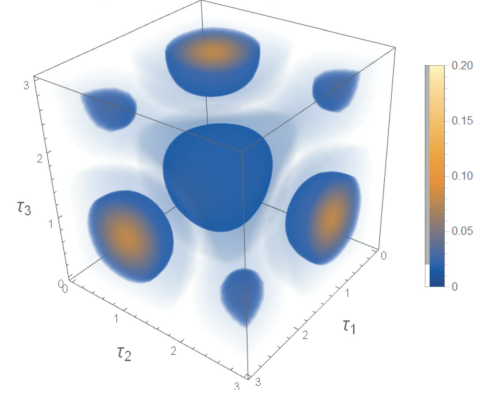


Fig. 8. Probability distribution of the three-photon output state $|3_\eta\rangle$ in (78).

VII. CONCLUSION

In this paper, we have studied the Tavis-Cummings model. Specifically, we have applied quantum linear systems theory to reveal typical features of the Tavis-Cummings model, the analytical expression has been derived for the output single-photon state of a Tavis-Cummings system in response to a single-photon input. We have also proposed a computational framework to derive the analytic form of the superposition state of the system and field. Note that the linear quantum systems' approach is only applicable when there is only one excitation. Future studies are to be done on subradiance and superradiance in the multi-excitation case.

APPENDIX

As concepts and properties of quantum linear passive systems are used in this paper, in particular Section IV, in this appendix we collect some of them for readability of this paper.

For the quantum linear system (13), from (18) we know the transfer function $G[s]$ is an *all-pass* function [44, pp. 357]. Actually, as shown in Remark 3.2, system (13) is passive. If we take expectation on both sides of (13) with respect to the initial joint system-field state (which is a unit vector in a Hilbert space), we get a *classical* linear system

$$\begin{aligned} \langle \dot{\bar{a}}(t) \rangle &= A \langle \bar{a}(t) \rangle + B \langle b_{\text{in}}(t) \rangle, \\ \langle b_{\text{out}}(t) \rangle &= C \langle \bar{a}(t) \rangle dt + \langle b_{\text{in}}(t) \rangle. \end{aligned} \quad (79)$$

Thus we can define controllability, observability, and Hurwitz stability for the quantum linear system (13) using those for the classical linear system (79).

Definition 7.1: The quantum linear passive system (13) is said to be *Hurwitz stable* (resp. *controllable*, *observable*) if the corresponding classical linear system (79) is *Hurwitz stable* (resp. *controllable*, *observable*).

The following result reveals the structure of quantum linear passive systems; see [29], [31] for more details.

Proposition 7.1: The quantum linear passive system (13) has the following properties.

- (i) Its Hurwitz stability, controllability and observability are equivalent to each other.
- (ii) It has only controllable and observable (*co*) subsystem and uncontrollable and unobservable ($\bar{c}\bar{o}$) subsystem. Moreover, each $\bar{c}\bar{o}$ subsystem is a closed (namely isolated) quantum system; see Eq. (21) and Corollary 3.1.
- (iii) Its poles corresponding to a $\bar{c}\bar{o}$ subsystem are all on the imaginary axis, while its poles corresponding to a *co* subsystem are on the open left half of the complex plane.

REFERENCES

- [1] R. H. Dicke, "Coherence in spontaneous radiation processes," *Physical Review*, vol. 93, no. 1, p. 99, 1954.
- [2] M. Tavis and F. W. Cummings, "Exact solution for an n -molecule—radiation-field hamiltonian," *Physical Review*, vol. 170, pp. 379–384, 1968.
- [3] M. A. Sillanpää, J. I. Park, and R. W. Simmonds, "Coherent quantum state storage and transfer between two phase qubits via a resonant cavity," *Nature*, vol. 449, no. 7161, pp. 438–442, 2007.
- [4] J. Majer, J. Chow, J. Gambetta, J. Koch, B. Johnson, J. Schreier, L. Frunzio, D. Schuster, A. A. Houck, A. Wallraff *et al.*, "Coupling superconducting qubits via a cavity bus," *Nature*, vol. 449, no. 7161, pp. 443–447, 2007.
- [5] J. M. Fink, R. Bianchetti, M. Baur, M. Göppl, L. Steffen, S. Filipp, P. J. Leek, A. Blais, and A. Wallraff, "Dressed collective qubit states and the tavis-cummings model in circuit QED," *Physical Review Letters*, vol. 103, p. 083601, 2009.
- [6] Z. Wang, H. Li, W. Feng, X. Song, C. Song, W. Liu, Q. Guo, X. Zhang, H. Dong, D. Zheng, H. Wang, and D.-W. Wang, "Controllable switching between superradiant and subradiant states in a 10-qubit superconducting circuit," *Physical Review Letters*, vol. 124, p. 013601, 2020.
- [7] T. Astner, S. Nevlacsil, N. Peterschofsky, A. Angerer, S. Rotter, S. Putz, J. Schmiedmayer, and J. Majer, "Coherent coupling of remote spin ensembles via a cavity bus," *Physical Review Letters*, vol. 118, no. 14, p. 140502, 2017.
- [8] G.-W. Deng, D. Wei, S.-X. Li, J. Johansson, W.-C. Kong, H.-O. Li, G. Cao, M. Xiao, G.-C. Guo, F. Nori *et al.*, "Coupling two distant double quantum dots with a microwave resonator," *Nano Letters*, vol. 15, no. 10, pp. 6620–6625, 2015.
- [9] D. J. van Woerkom, P. Scarlino, J. H. Ungerer, C. Müller, J. V. Koski, A. J. Landig, C. Reichl, W. Wegscheider, T. Ihn, K. Ensslin, and A. Wallraff, "Microwave photon-mediated interactions between semiconductor qubits," *Physical Review X*, vol. 8, p. 041018, 2018.
- [10] B. Wang, T. Lin, H. Li, S. Gu, M. Chen, G. Guo, H. Jiang, X. Hu, G. Cao, and G. Guo, "Correlated spectrum of distant semiconductor qubits coupled by microwave photons," *Science Bulletin*, vol. 66, no. 4, pp. 332–338, 2021.
- [11] M. Gross and S. Haroche, "Superradiance: An essay on the theory of collective spontaneous emission," *Physics Reports*, vol. 93, no. 5, pp. 301–396, 1982.
- [12] Q.-M. Chen, Y.-x. Liu, L. Sun, and R.-B. Wu, "Tuning the coupling between superconducting resonators with collective qubits," *Physical Review A*, vol. 98, p. 042328, 2018.
- [13] W.-L. Li, G. Zhang, and R.-B. Wu, "The dynamical model of flying-qubit control systems," in *20th IFAC World Congress*, vol. 50, no. 1, 2020, pp. 11 755–11 759.
- [14] Y. Pan and G. Zhang, "Scattering of few photons by a ladder-type quantum system," *Journal of Physics A: Mathematical and Theoretical*, vol. 50, no. 34, p. 345301, 2017.
- [15] J. E. Gough and M. R. James, "The series product and its application to quantum feedforward and feedback networks," *IEEE Transactions on Automatic Control*, vol. 54, no. 11, pp. 2530–2544, 2009.
- [16] J. Combes, J. Kerckhoff, and M. Sarovar, "The SLH framework for modeling quantum input-output networks," *Advances in Physics: X*, vol. 2, no. 3, pp. 784–888, 2017.
- [17] C. Gardiner and P. Zoller, *Quantum Noise: A Handbook of Markovian and Non-Markovian Quantum Stochastic Methods with Applications to Quantum Optics*. Springer Science & Business Media, 2004, vol. 56.
- [18] H. M. Wiseman and G. J. Milburn, *Quantum Measurement and Control*. Cambridge university press, 2010.
- [19] J. Zhang, Y.-X. Liu, R.-B. Wu, K. Jacobs, and F. Nori, "Quantum feedback: theory, experiments, and applications," *Physics Reports*, vol. 679, pp. 1–60, 2017.
- [20] R. Loudon, *The Quantum Theory of Light*. OUP Oxford, 2000.
- [21] G. J. Milburn, "Coherent control of single photon states," *The European Physical Journal Special Topics*, vol. 159, no. 1, pp. 113–117, Jun 2008.
- [22] S. Fan, S. E. Kocabas, and J. T. Shen, "Input-output formalism for few-photon transport in one-dimensional nanophotonic waveguides coupled to a qubit," *Physical Review A*, vol. 82, p. 063821, 2010.
- [23] J. E. Gough, M. R. James, H. I. Nurdin, and J. Combes, "Quantum filtering for systems driven by fields in single-photon states or superposition of coherent states," *Physical Review A*, vol. 86, no. 4, p. 043819, 2012.
- [24] G. Zhang and M. R. James, "On the response of quantum linear systems to single photon input fields," *IEEE Transactions on Automatic Control*, vol. 58, no. 5, pp. 1221–1235, 2013.
- [25] J. E. Gough and G. Zhang, "Generating nonclassical quantum input field states with modulating filters," *EPJ Quantum Technology*, vol. 2, pp. 2–15, 2015.
- [26] Y. Pan, G. Zhang, and M. R. James, "Analysis and control of quantum finite-level systems driven by single-photon input states," *Automatica*, vol. 69, pp. 18–23, 2016.
- [27] Y. Pan, D. Dong, and G. Zhang, "Exact analysis of the response of quantum systems to two photons using a QSDE approach," *New Journal of Physics*, vol. 18, pp. 033004, 2016.
- [28] A. O. Davis, V. Thiel, M. Karpiński, and B. J. Smith, "Measuring the single-photon temporal-spectral wave function," *Physical Review Letters*, vol. 121, no. 8, p. 083602, 2018.
- [29] J. E. Gough and G. Zhang, "On realization theory of quantum linear systems," *Automatica*, vol. 59, pp. 139–151, 2015.
- [30] H. I. Nurdin and N. Yamamoto, *Linear Dynamical Quantum Systems: Analysis, Synthesis, and Control*, Springer, 2017.
- [31] G. Zhang, S. Grivopoulos, I. R. Petersen, and J. E. Gough, "The Kalman decomposition for linear quantum systems," *IEEE Transactions on Automatic Control*, vol. 63, no. 2, pp. 331–346, 2018.
- [32] G. Zhang, I. R. Petersen, and J. Li, "Structural characterization of linear quantum systems with application to back-action evading measurement," *IEEE Transactions on Automatic Control*, vol. 65, pp. 3157–3163, 2020.
- [33] G. Zhang and M. R. James, "Direct and indirect couplings in coherent feedback control of linear quantum systems," *IEEE Transactions on Automatic Control*, vol. 56, pp. 1535–1550, 2011.
- [34] N. Yamamoto, "Decoherence-free linear quantum subsystems," *IEEE Transactions on Automatic Control*, vol. 59, no. 7, pp. 1845–1857, 2014.
- [35] F. Ticozzi and L. Viola, "Quantum markovian subsystems: invariance, attractivity, and control," *IEEE Transactions on Automatic Control*, vol. 53, no. 9, pp. 2048–2063, 2008.
- [36] Y. Wang, J. Minář, L. Sheridan, and V. Scarani, "Efficient excitation of a two-level atom by a single photon in a propagating mode," *Physical Review A*, vol. 83, no. 6, p. 063842, 2011.
- [37] A. Blais, A. L. Grimsmo, S. M. Girvin, and A. Wallraff, "Circuit quantum electrodynamics," *Review of Modern Physics*, vol. 93, p. 025005, 2021.
- [38] M. Pierre, I.-M. Svensson, S. Raman Sathyamoorthy, G. Johansson, and P. Delsing, "Storage and on-demand release of microwaves using superconducting resonators with tunable coupling," *Applied Physics Letters*, vol. 104, no. 23, p. 232604, 2014.
- [39] K. A. Fischer, L. Hanschke, J. Wierzbowski, T. Simmet, C. Dory, J. J. Finley, J. Vučković, and K. Müller, "Signatures of two-photon pulses from a quantum two-level system," *Nature Physics*, vol. 13, no. 7, pp. 649–654, 2017.
- [40] K. A. Fischer, R. Trivedi, V. Ramasesh, I. Siddiqi, and J. Vučković, "Scattering into one-dimensional waveguides from a coherently-driven quantum-optical system," *Quantum*, vol. 2, p. 69, 2018.
- [41] R. Trivedi, K. Fischer, S. Xu, S. Fan, and J. Vuckovic, "Few-photon scattering and emission from low-dimensional quantum systems," *Physical Review B*, vol. 98, no. 14, p. 144112, 2018.
- [42] W. J. Rugh, *Linear System Theory*. Prentice-Hall, Inc., 1996.
- [43] O. O. Chumak and E. V. Stolyarov, "Photon distribution function for propagation of two-photon pulses in waveguide-qubit systems," *Physical Review A*, vol. 90, p. 063832, 2014.
- [44] K. Zhou, J. Doyle, and K. Glover, *Robust and Optimal Control*, Upper Saddle River, NJ:Prentice-Hall, 1996.